Review

TiO$_2$ assisted photocatalysts for degradation of emerging organic pollutants in water and wastewater

Hugues Kamdem Paumo [a,*], Sadou Dalhatou [b], Lebogang Maureen Katata-Seru [a,*], Boniface Pone Kamdem [c], Jimoh Oladejo Tijani [d], Venkataraman Vishwanathan [e], Abdoulaye Kane [f], Indra Bahadur [a,*]

[a] Department of Chemistry, Faculty of Natural and Agricultural Sciences, North-West University, Mafikeng 2735, South Africa
[b] Département of Chemistry, Faculty of Science, University of Maroua, P.O. Box 814, Maroua, Cameroon
[c] Department of Pharmacy, Faculty of Pharmaceutical Sciences, University of Sao Paulo, Brazil
[d] Department of Chemistry, Federal University of Technology, Minna, Nigeria
[e] Applied Sciences Department, Faculty of Engineering and Applied Sciences, Botho University, Gaborone, Botswana
[f] UniLaSalle-Ecole des Métiers de l'Environnement, Campus de Ker Lann, avenue Robert Schuman, 35170 Bruz, France

ARTICLE INFO

ABSTRACT

The occurrence of emerging organic pollutants (EOPs) in the aquatic environment originating from point and diffuse sources, has been the subject of global apprehension in the recent years. These groups of compounds include pharmaceuticals, industrial products/by-products, personal care products and pesticides, which demonstrated pseudo-persistence conduct, resistance to degradation and frequent entrance into the environment through wastewater. The effective removal of EOPs from industrial wastewater and sewage represents one strategic procedure that could diminish their intrinsic environmental impacts. For this purpose, the advanced oxidation treatment using heterogeneous photocatalysts under light irradiation is consistently argued to show potential as economically viable and commercially feasible technology. Remarkably, for the efficient degradation of EOPs, nanostructured titanium dioxide (TiO$_2$) containing materials have been favoured because of their anticipated combination of unique electronic structure, impressive light absorption properties, prolonged excited-state lifetimes and enhanced charge transport features. This review first highlights the research efforts associated with the manifestation and toxicity of EOPs in the environment. Subsequently, the treatment technologies that have been utilized in the literature for the removal of EOPs from aqueous media are summarized. Background information on the fundamental principles of light-driven catalytic activity at the surface of semiconductors is also presented. Next, a systematic survey of the latest progress in the development of TiO$_2$ photocatalystsfor the degradation of EOPs is elaborated. The contribution of TiO$_2$ photocatalysis in hybrid advanced oxidation procedures is also discussed. Notwithstanding the scientific efforts toward the minimization of wastewater generation, specific waste conditioning, and important information regarding cost, and benefits, as well as the scale-up of the treatment procedure are required to complement the advanced oxidative processes (AOPs).

© 2021 Elsevier B.V. All rights reserved.

Contents

Abbreviations: EOPs, Emerging organic pollutants; UNESCO, United Nations Educational, Scientific and Cultural Organization; IHP, International Hydrological Programme; SPR, Surface plasmon resonance; BPA, Bisphenol A; HaCaT, Human keratinocyte cells; LC$_{50}$, Concentration of the pollutant which is lethal to 50% of a targeted population; DDT, Dichlorodiphenyl trichloroethane; PEPCK, Phosphoenol pyruvate carboxykinase; UV, Ultraviolet; AOPs, Advanced Oxidation Processes; CB, Conduction band; VB, Valence band; TTIP, Titanium tetraisopropoxyde; rGO, Reduced graphene oxide; NSAIDs, Non-steroidal anti-inflammatory drugs.
 * Corresponding authors.
   E-mail addresses: kamdem_hugues@yahoo.com (H.K. Paumo), lebo.seru@nwu.ac.za (L.M. Katata-Seru), bahadur.indra@nwu.ac.za (I. Bahadur).

1. Introduction

1.1. Background

Rapid industrial development, agricultural revolution, and population density has led to an increase in environmental pollution which is now regarded as a global crisis. This issue originates from the consistent improvement in the standard of living and increasing consumer demands [1]. Adding to this alarming situation, the global demands for water as the most vital of all natural resources are also growing [2]. Yet, there is a continuous decline in the quality of the freshwater habitats owing to the presence of a significant number of emerging contaminants. Safeguarding water quality is essential for human development and well-being. In this perspective, the UNESCO International Hydrology Programme has highlighted recently, the urgent need to balance the human well-being and environmental risk associated with exposure to emerging pollutants in water [3]. In particular, the emerging organic pollutants (EOPs) are organic compounds that are presently not enclosed by existing water-quality legislation, but have been identified or mistrusted to exhibit adverse effects on human health and the environmental ecosystems. These pollutants include pharmaceuticals, pesticides, personal care products, perfluorinated compounds, heavy metals and industrial products/by-products [4,5]. Although encountered in the environment at very low concentrations, the detection of EOPs has been ascribed to improve detection sensitivity of the advanced analytical technologies.

Pharmaceuticals like non-steroidal anti-inflammatory drugs (NSAIDs), antibiotics, analgesics and disinfectants, have often been reported in surface water in concentrations that range from ng/L-μg/L [6–8]. Water pollution from pharmaceuticals is alleged to arise either from the intensive livestock husbandry and aquaculture or from sewage and septic systems (Fig. 1). Remarkably, recent studies revealed that pharmaceuticals and personal care products are not totally removed at sewage treatment plants [9]. An illustrative example is the investigation carried by Rimayi and co-workers in the Hartbeespoort Dam catchment, Gauteng, South Africa [10]. Findings from this study uncovered up to 15 compounds of emerging concern belonging to steroid hormones, pharmaceuticals and pesticides.

In addition, pesticides applied to boost the yield of crops, and preserve farm products and meet global food demands also constitute a serious health risk to humans. A recent survey indicates high concentrations of pesticide residues in waterbodies. Approximately one-third of all harvested global agricultural products have been linked to application of pesticides. However, inappropriate application and disposal of pesticides often resulted in environmental pollution. A recent study in Tanzania revealed the presence of different pesticide residues in ground and surface water [11].

Phenolic compounds, which are widely employed as industrial organic chemicals to produce insecticides, coatings, dyes and many more, are also often detected in the aquatic environments [12]. Such compounds include bisphenol A (BPA) which is extensively employed in consumer and industrial products, has been identified as an emerging organic pollutant following the risk assessments. In 2011, this synthetic organic compound was one of the most industrialized chemicals around the world, with a production of more than 5 million tons [13]. In addition, according to a report by Transparency Market Research, the global demand for this environmental contaminant is anticipated to rise at an annual rate of 5.4% from 2013-2019 [14]. BPA serves as a monomer for the generation of polycarbonate plastics or epoxy resin, and has also
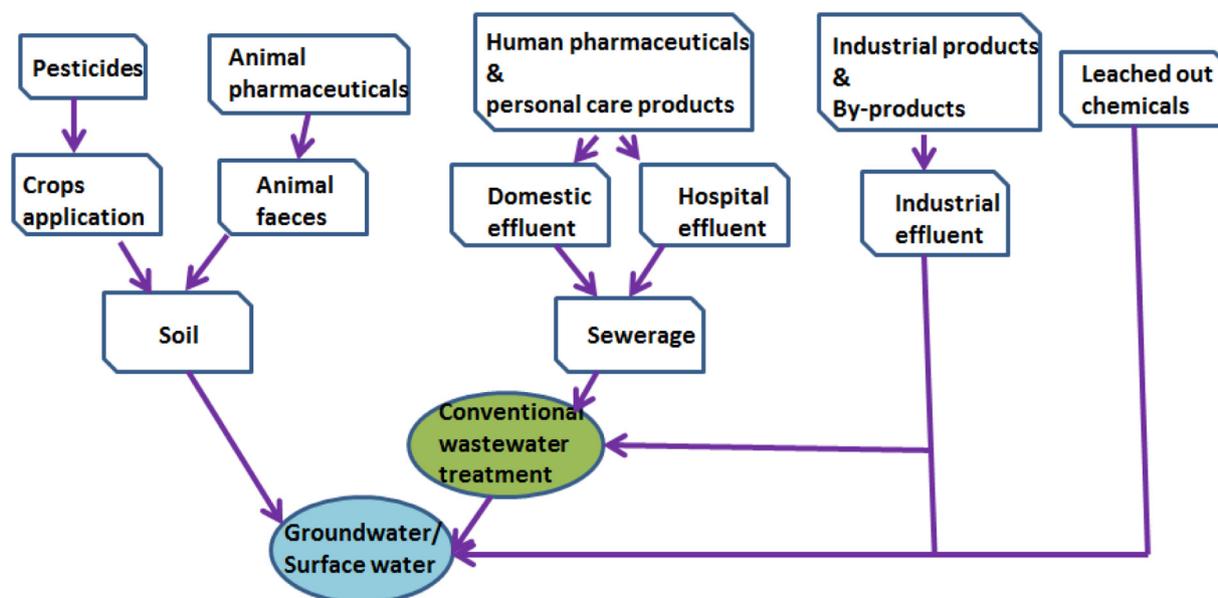

Fig. 1. Schematic paths of EOPs in the environment

been found to leach from BPA-containing products [15–18]. Though some of the pharmaceuticals (encountered in relatively lower concentration) are not be expected to display acute toxicity, they are bio-accumulative in the receiving effluents and thereby predisposed to synergistic toxicity. Hence, there have recently been significant research interests in exploring the biological effects of EOPs.

This article sets out to expose the detrimental effects of EOPs in our environment and the treatment technologies that have been employed in the literature for their remediation in aqueous milieu. Information on the basic principles of light-driven catalytic activity at the surface of special materials is presented as a highly appreciated technique. Since TiO_2 is one of the most frequently reported materials in water treatment, a methodical investigation of the latest advancement in the development of TiO_2-based photocatalysts and their contribution in hybrid advanced oxidation procedures is described. A critical assessment section provides the authors' suggestions for a better alternative outlook.

1.2. Environmental and health risks associated with EOPs

There are many EOPs which pose serious environmental and health risks. BPA (Fig. 2), for example, is an endocrine disruptor that has the potential to imitate the naturally occurring hormones such as androgens and estrogens. Endocrine disrupting compounds act by interfering with the intracellular receptors whose role is to regulate gene expression [19]. Endocrinology investigation in CD-1(cluster of differentiation 1) mice exposed to BPA revealed several adverse effects, including, a modification in the growth of mammary gland in female foetuses, a reduced level of testosterone in male, a spread of basal cells accountable for the development of prostate cancer and an upsurge in the number of abnormal sperms [20,21]. BPA has also demonstrated a substantial level of *in vitro* and *in vivo* cell toxicities. Recently, the *in vivo* neurotoxicity of BPA revealed that even at relatively low dose, this compound has the potential to affect the brain cells, leading to inferior memory storage [22].

The aquatic toxicity of phenol and its methylated derivatives (cresols) has also been reviewed recently by Duan and co-workers [12]. According to the data presented in that literature survey, the effects of phenol and cresols to marine organisms range from the inhibition of bacteria bioluminescence to the mortality in fish species. *Cirrhinus mrigala* well-known as the white carp, was found to exhibit a higher sensitivity to phenol in the aquatic medium, with the LC_{50} value of 1.555 mg/L after 96 h exposure time. Park et al. [23] observed a decline in the leaf growth, and colony integrity of the macrophyte *Lemna paucicostata* exposed to 11.4 and 22.8 μM phenol for 72 h at 25 °C, respectively. Findings from this study also displayed that the toxicity observed was due to the annihilation of chlorophylls and reduction of photosynthetic activity.

Dichloro-diphenyl-trichloroethane
(**DDT**)

7-Chloro-1,3-dihydro-3-hydroxy-5-phenyl-1,4-benzodiazepin-2-one
(**Oxazepam**)

5-Chloro-2-(2,4-dichlorophenoxy)phenol
(**Triclosan**)

1-cyclopropyl-6-fluoro-4-oxo-7-piperazin-1-ylquinoline-3-carboxylic acid
(**Ciprofloxacin**)

2-{4-[2-(4-Chloro-benzoylamino)-ethyl]-phenoxy}-2-methyl-propionic acid
(**bezafibrate**)

[2-(2,6-Dichloro-phenylamino)-phenyl]-acetic acid
(**Diclofenac**)

2,2-Bis(4-hydroxyphenyl)propane
(**BPA**)

2-(4-Isobutyl-phenyl)-propionic acid
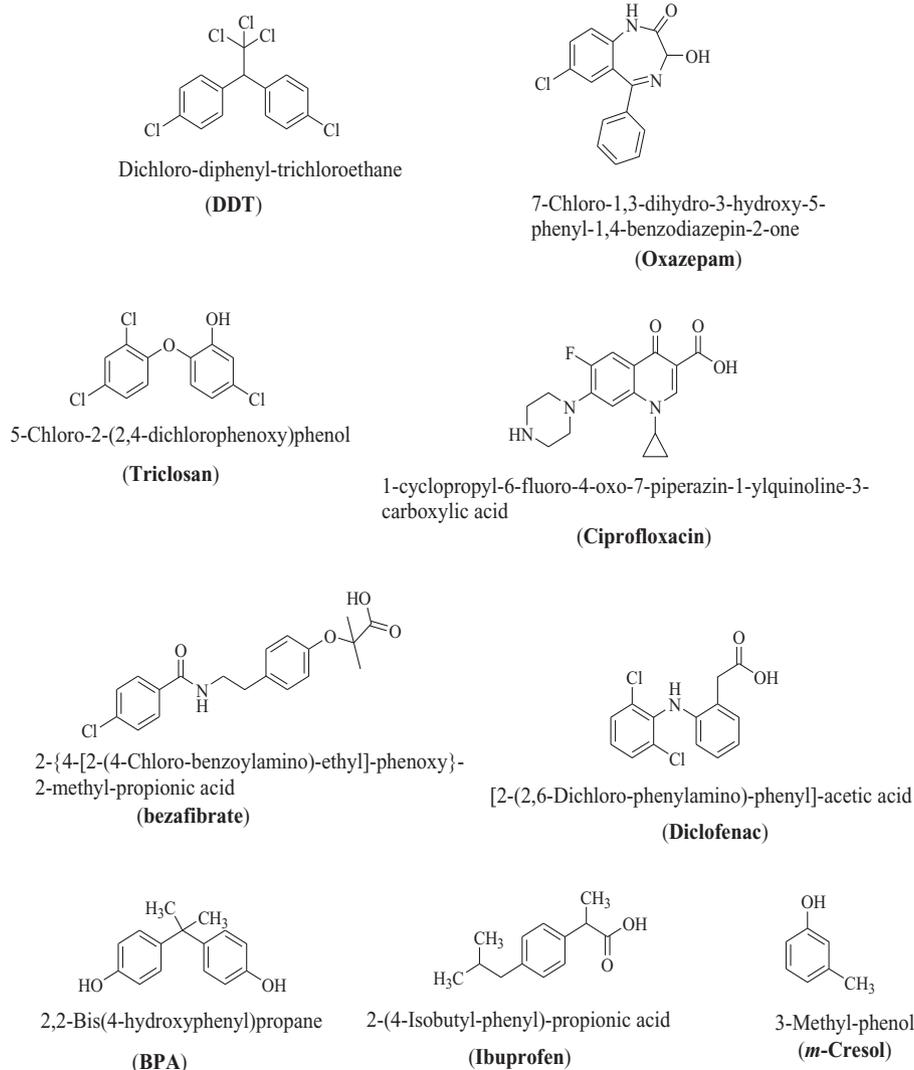(**Ibuprofen**)

3-Methyl-phenol
(***m*-Cresol**)

Fig. 2. Structural formula of selected EOPs

Environmental pollution triggered by the presence of pharmaceuticals in sewage effluents, has equally raised anxieties in the scientific community. The occurrence of antibiotics and personal care products in the environment is well-reported to induce the influx of antibiotic resistance pathogenic microbes, the genotoxicity in aquatic species, and the disruption of ecological processes and functions [24,25]. For instance, a recent characterisation of the effluent of the Gabriel Montpied hospital, France, revealed the incidence of ciprofloxacin-resistant microorganisms [26]. The toxic threat of this fluoroquinolone derivative during that investigation was assessed and the hazard quotient was evaluated to be 2.08, indication for a budding hazard [27]. Markedly, ciprofloxacin is among the most prescribed antibiotics in French hospitals. Pertaining to the genotoxicity of pharmaceuticals, the zebrafish embryos and larvae, for example, have previously been found to experience significant genetic toxicity after exposure to triclosan (an antibacterial compound found in a variety of personal care commodities) [22]. On the other hand, Brodin et al. reported a modification in the activity and feeding behaviour of animal species in oxazepam-contaminated water [28]. The presence of this psychoactive agent, even at lower concentration (1.8 μg/L), resulted in high locomotion and feeding rate of redfin perch. Likewise, a strong correlation has been established between the rate at which zooplankton population decrease and the presence of NSAID ibuprofen in water bodies [29].

Several pesticides have also demonstrated endocrine disrupting activity. Zhang et al. [30], for example, reported the repression of intracellular glucocorticoid receptor transactivation and the inhibition of phosphoenolpyruvate carboxykinase (PEPCK) gene expression in rat hepatoma cells treated with dichlorodiphenyltrichloroethane (DDT) analogues. This organochlorine compound has been utilized for insect control in crop and livestock production [31]. The glucocorticoid receptor is a ligand-activated transcriptional regulatory factor involved in the control of several physiological processes [32]. On the other hand, PEPCK is a rate-controlling enzyme of glycolysis, expressed in the kidney, liver and muscle [33].

A computer-based modeling approach has also been used to screen and evaluate the effect of EOPs on the biological system through structure-activity relationships (SAR). A well-known example of a mechanism-based SAR application that has influenced risk assessment is the modeling of aryl hydrocarbon (Ah) receptor-binding capability of polyhalogenated aromatic compounds [34]. These are known to produce biological reactions *via* an enzymatic receptor-mediated response, followed by genetic induction. The structural similarity between EOPs and biological molecules enables them to bind at the enzyme active site, creating malfunction in the biological system [35]. An illustration is the structural resemblance between polychlorinated biphenyls/polybrominated diphenyl ethers and thyroid hormones [T3 (triiodothyronine) and T4 (thyroxine)]. These organic contaminants are predicted through SAR to persuade thyroid hormone disruption. In order to lessen the eco-toxicological risk associated with the presence of EOPs in water sources, innovative wastewater treatment methodologies have been proposed in the literature and these are discussed in the following section.

2. Methods for the removal of EOPs from water

Investigations of the fate of EOPs in wastewater treatment using methods such as coagulation-flocculation and sedimentation have shown their limitations. These technological processes only afford the removal of solids and oils. Other methodologies, including adsorption and biological treatment, have also demonstrated promising potential for the reduction of soluble organic hazards in water.

2.1. Adsorption, membrane filtration and biological treatment technologies

Adsorption technology has been reported for the removal of EOPs by utilizing specific materials having high surface area and surface functional groups that are able of binding with the organic contaminants. Some of the common adsorbents include clay, zeolite, metal oxides, polymeric and carbon-based materials [36–39]. For example, Jin et al. [40] reported the synthesis of Fe_3O_4-decorated reduced graphene oxides as promising adsorbent for the removal of endocrine-disrupting chemicals from wastewater. The prepared material exhibited maximum adsorption capacities of 48 and 63 mg/g at 293 °K for the removal of BPA and 4-nonylphenol, respectively. Activated carbon is another commonly used adsorbent for wastewater treatment owing to its relatively higher specific surface area (>800 m^2/g), grain size and porous structure. This adsorbent is well-suited for the removal of polar compounds. Previously, Bautista-toledo and his group also reported the use of activated carbon from different sources in BPA adsorption from aqueous matrix [41]. The tested adsorbents demonstrated maximum adsorption capability of 263 mg/g at 298 °K. The ability of carbon-based materials to effect the adsorption of EOPs from water has been attributed to π-π stacking between the benzene rings of the adsorbent-adsorbate system [42]. Das et al. described the reduction of 4 nitrophenol using the magnetic polypyrrole-mercaptoacetic acid loaded with silver nanoparticles [43]. The pseudo-first-order reduction rate constant was ascertained as 14.3×10^{-2} min^{-1} with 7.5 mg of this adsorbent. Although, adsorption technology has been established as alternative method for the removal of EOPs, the adsorbent performance depends entirely on the use of fresh material or recurrent regeneration of the spent adsorbent [44,45]. In most cases, the adsorbents are not reusable or regenerable after a few turnover cycles. This is attributed to the repeated desorption procedure that leads to loss of active binding sites
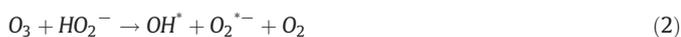
Membrane filtration is another technology that has also been applied successfully for EOPs uptake from water. In this process, a micro-porous layer acts as a barrier for the restriction of inorganic particles, organic colloids, and dissolved organic pollutants. There are different types of technology in membrane filtration for wastewater remediation. These include micro- and ultra-filtration (MF & UF). The membranes have minute pore sizes anywhere in the range between 1×10^{-2} to 4×10^{-2} μm. For example, ceramic membranes consisting of mixed oxides of titanium and zirconium (TiO_2 and ZrO_2), produced with a wide range of superficial porosity, have been reported for the effective removal of BPA from biologically pre-treated water samples through micro- and nano-filtration [46]. However, during this investigation, the membranes permeate flux were found to decline with time because of fouling. Adsorption of hydrophobic organic contaminants like BPA onto the membranes could impact their hydrophobicity and thereby their filtration capacity over time. Membranes with lower fouling potential like forward osmosis membranes have equally been described for EOPs elimination in contaminated effluents [47,48]. Forward osmosis is based on the spontaneous diffusion of water across a semi-permeable membrane and the rejection of contaminants. This process is dependent on the osmotic pressure gradient across the membrane. Even though forward osmosis can limit operational problems such as fouling, the concentration polarization phenomenon is known to substantially reduce the effectual osmotic pressure across the forward osmosis membranes [49].

Another reported approach for the abatement of EOPs in wastewater is the bioremediation. It is based on the ability of selected naturally occurring microorganisms to interact with organic contaminants in water body. This type of initiative opens a sustainable treatment of EOPs in compliance with stringent socio-environmental regulations. This technique is more often described as cost-effective approach that is based upon the metabolic potential of some microorganisms to reverse the adverse effects of EOPs. For example, Martins et al. recently identified Gram-negative sulfate-reducing bacteria *Desulfovibrio* as anaerobic microorganism with the predisposition to remove antibiotic ciprofloxacin in aqueous medium [50]. Similarly, fungus *Aspergillus versicolor* was found to exhibit biodegradation towards pesticide triclosanin synthetic wastewater and inferred chloride ions as the

ultimate product [51]. Although highly valued, bioremediation technique is also related with shortcomings like lower bioavailability of EOPs on temporal and/or spatial scales and lack of benchmark reports for efficiency assessment [52]. These shortcomings and the incapacity of the biological treatment technologies to efficiently remove EOPs from wastewater have paved the way for the development of chemical-oxidative methods.

2.2. Chemical-oxidative degradation

Chemical oxidation is a treatment approach that utilizes oxidizing agents to chemically transform EOPs into less toxic products. The most frequently used and reported oxidants include ferrate(VI) (FeO_4^{2-}), hydrogen peroxide (H_2O_2) and ozone (O_3). For example, Sailo et al. utilized FeO_4^{2-} for the degradation of BPA and NSAID diclofenac in aqueous solution [53]. Similarly, Quero-Pastor and co-workers reported the use of O_3 for the decomposition of NSAID ibuprofen in water [54]. Ozone is obtained *via* dissociation of molecular oxygen and binding of the produced free O atoms with other available O_2. Following their formation, O_3 in aqueous solution swiftly undergoes interaction to afford the highly reactive species like hydroxyl radical ($OH^{\bullet}$), superoxide ($O_2^{\bullet-}$) and peroxyl ($OOH^{\bullet}$), as depicted in the following equations [55,56].

$$O_3 + OH^- \rightarrow HO_2^- + O_2 \tag{1}$$

$$O_3 + HO_2^- \rightarrow OH^* + O_2^{*-} + O_2 \tag{2}$$

$$O_3 + OH^* \rightarrow OOH^* + O_2 \tag{3}$$

These generated radicals display strong oxidation potential and can instantly degrade or mineralize EOPs into CO_2 and water in wastewater.

Ozonation has also been combined with light irradiation (UV/Visible), H_2O_2 and/or a catalyst to improve the EOPs degradation process. For example, the oxidative degradation of a series of EOPs, including, pharmaceuticals and herbicides in groundwater/surface water sample has been reported by Yao et al. [57] using O_3 under ultraviolet (UV) light irradiation. Another descriptive example is the degradation of 23 pharmaceuticals present in micro-filtered water sample of an urban wastewater treatment plant in Gran Canaria, Spain [58]. This was achieved by employing H_2O_2 under UV irradiation. The high-energy photons emitted by UV light was capable of persuading homolytic fission of H_2O_2 molecules to produce secondary oxidant $^{\bullet}OH$ radicals (Eq. 4). These photons promoted the decomposition of O_3 to release molecular oxygen and atomic oxygen in singlet D state (Eq. 5) [59]. The latter may then interact with water molecules to generate •OH free radicals (Eq. 6).

$$H_2O_2 \overset{h\nu}{\rightarrow} 2OH\bullet \tag{4}$$

$$O_3 \overset{h\nu}{\rightarrow} O_2 + O(^1D) \tag{5}$$

$$H_2O + O(^1D) \rightarrow 2OH\bullet \tag{6}$$

Fenton and photo-assisted Fenton techniques are advanced oxidation processes (AOPs) that evolved from the activity of H_2O_2 in the presence of iron species. These have also been exploited for the effective decomposition of EOPs in aqueous media. Santos et al. [60], for example, reported up to 55% mineralization of fluoroquinolone norfloxacin in Fenton oxidation process, using $H_2O_2/FeSO_4.7H_2O$ ratio of 5.64/0.8 at pH 3. The mechanism of EOPs degradation using this method initiates *via* OH• formation through sequential reactions of Fe^{2+} and Fe^{3+} with H_2O_2, as shown in Eq. 7 and 8 [61–63]. However, one of the limitations of this system is the fact that at neutral pH, precipitation of ferric hydroxide occurs and reduced amount of dissolved iron are available [24,64,65]. Furthermore, this water treatment technique also suffers from the difficulty in recycling the homogeneous catalysts.

$$Fe^{2+} + H_2O_2 \rightarrow Fe^{3+} + OH^- + OH^* \tag{7}$$

$$Fe^{3+} + H_2O_2 \rightarrow Fe^{2+} + H^+ + OOH^* \tag{8}$$

Recent literature on water treatment procedure also promotes the persulfate-based AOPs [66,67]. This technology is based on the release of a large amount of sulfate radicals ($SO_4^{\bullet-}$) by homolytic or heterolytic peroxide bond cleavage of the peroxymonosulfate and peroxydisulfate molecules. $SO_4^{\bullet-}$ also possesses a strong oxidizing capability and interacts with organic pollutants through electron transfer mechanism. Although this chemical-oxidative degradation procedure is being described as viable alternative to H_2O_2-based processes, it is also associated with limitations such as selective degradation of organic pollutants and production of undesirable byproducts in real water media.

Another AOP of particular attention is the use of photosensitive solid material for EOPs remediation in water bodies. This light-driven catalytic activity at a solid-liquid interface, referred as heterogeneous photocatalysis is also capable of complete decomposition/mineralization of the organic contaminants.

2.3. Heterogeneous photocatalysis

Heterogeneous photocatalysis is a treatment technology that involves the use of semiconductors, having the ability of being activated under light irradiation for redox reactivity [68,69]. This method offers several advantages in environmental remediation as it is an eco-friendly technology with minimum secondary pollution and no regeneration step for multiple cycles of reuse. During heterogeneous photocatalytic activity for EOPs abatement in water medium, five steps have been established to take place [70] and these include:

(i) the diffusion of EOPs from the dissolved aqueous matrix to the catalyst surface,
(ii) their sorption, based upon the surface atomic arrangement and coordination.
(iii) the light irradiation-induced chemical transformation at the surface of the semiconductor catalyst,
(iv) the release of the degradation products from the surface of the semiconductor catalyst,
(v) and the release of these products from the boundary layer to the bulk of the aqueous matrix.

The importance of EOPs pre-adsorption at the photocatalyst surface can be uncovered using the Langmuir-Hinshelwood (L-H) kinetics model, adapted to elucidate the interactions at a solid-liquid interface. According to this model, the reaction rate at the interface is determined by the concentration of targeted organic pollutant and the apparent adsorption equilibrium constant, as expressed in the following equation [71]:

$$r = -\frac{dC}{dt} = Kr\frac{Kc}{1 + Kc} \tag{9}$$

where K_r and K are the apparent reaction rate constant and apparent binding constant, respectively. Considering the low concentration of EOPs in water bodies, and consequently in heterogeneous photodegradation studies, Eq. 9 can be reduced to the decay kinetics with an apparent reaction rate constant $K_{app.}$

$$-\frac{dC}{C} = KrKdt = K_{app}dt \tag{10}$$

The integration of Eq. 10 gives:
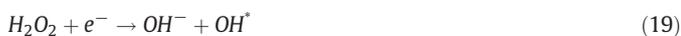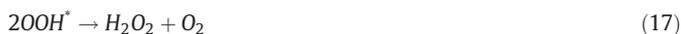
$$Ln\left(\frac{C_o}{C}\right) = K_{app}t \tag{11}$$

where C_o is the initial concentration. K_{app} can be determined from the slope of the linear graph of $ln(C_0/C)$ *versus* decay time t.

Upon irradiation of a semiconductor suspended in aqueous medium with light bearing energy equal or greater than that of its band gap (Eg), there is an instigation of excitation of valence band (VB) electrons (e⁻), and formation of holes (h⁺) (Fig. 3).

A fundamental conduction transpires in light illumination *via* the positively charged holes (h⁺) in the VB and electrons (e⁻) in the CB (Eq. 12).

$$TiO_2 \, in \, \lambda \leq 390nm \rightarrow e-h(exciton) \rightarrow e^- + h^+ \tag{12}$$
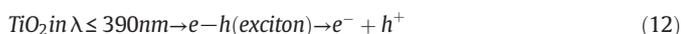
Once generated, the charge carriers (e⁻/h⁺) may move from the bulk to the semiconductor surface and ultimately initiate several reactions [73]. Hence, the overall efficiency of a semiconductor to act as a catalyst for the light-driven transformation of organic contaminants in aqueous environment strongly depend on the potential of generated e⁻/h⁺ charge carriers to produce the active radicals. The reaction of water molecules or adsorbed hydroxyl ions (OH⁻) with h⁺ generates OH• radicals are shown in (Eq. 13 and 14). On the other hand, adsorbed oxygen molecules (O_2) interact with photoexcited electrons to produce $O_2^{•-}$ radicals (Eq. 15). The sequence of reactions that occur at the surface of photoactivated catalyst for the formation of active radicals is shown as follows [74,75]:

$$h^+ + H_2O \rightarrow OH^* + H^+ \tag{13}$$

$$h^+ + OH^- \rightarrow OH^* \tag{14}$$

$$e^- + O_2 \rightarrow O_2^{*-} \tag{15}$$

$$O_2^{*-} + H^+ \rightarrow OOH^* \tag{16}$$

$$2OOH^* \rightarrow H_2O_2 + O_2 \tag{17}$$

$$H_2O_2 + O_2^{*-} \rightarrow OH^- + OH^* + O_2 \tag{18}$$

$$H_2O_2 + e^- \rightarrow OH^- + OH^* \tag{19}$$

It is evident that charge carriers interaction upon one another (recombination) is detrimental to the performance of a catalyst involved in photo-assisted activity. This phenomenon occurs when an excited electron drops back to the VB through a radiative or non-radiative process [76]. The charges reunion can take place either at the surface or in
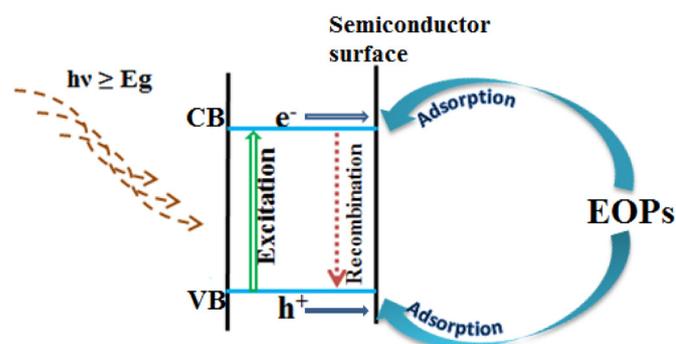

Fig. 3. Illustrative diagram of the photoexcitation of a semiconductor with suitable light [72]

the bulk of the catalyst and this process is controlled by the e⁻/h⁺ charge carriers mobility or trapping, the density of defects in the semiconductor lattice, and the existence of an interfacial charge carrier transfer [73,77]. It is worth noting that the density functional theory (DFT) calculations have foreseen oxygen vacancy sites and metal interstitials as the donor-centers accounting for n-type conductivity, while metal cation vacancies are acceptor-centers responsible for p-type conductivity [78]. With regard to TiO_2, this computer-based modeling techniquealso indicates that the presence of Ti^{3+} vacancies triggers ferromagnetism.

Numerous semiconductors have been investigated in photocatalytic degradation of EOPs in wastewater. These include ZnO, MoO_3, ZnS, CdS, ZrO_2, WO_3, CdSe, SnO_2 and TiO_2 [79–85].

TiO_2, also known as titania, is a low-cost and environmentally benign oxide that has gained commercial success in cosmetic, beauty and personal care applications [86]. Moreover, interest in TiO_2-containing catalysts for the light-driven abatement of organic contaminants in wastewater has been tremendous since the early report by Frank and Bard [87]. Owing to its inherent oxygen vacancy, TiO_2 is typically an n-type semiconducting material with the VB and CB edges mainly originating from oxygen 2p-orbitals and titanium 3d-orbitals, respectively [88–90]. TiO_2 photocatalysis depends on variables like the crystallinity, specific surface area, and surface hydroxyl groups of the TiO_2 catalyst. This distinctive material presents relatively polar surfaces that allow for ease adsorption of hydrophilic pollutants.

3. TiO₂ crystalline structure and the facets exposed

TiO_2 exhibits three main semiconducting polymorphs, namely, brookite, rutile, and anatase. Anatase and rutile phases are distinguished by a tetragonal symmetry, whereas brookite is characterized by an orthorhombic crystal system. However, the ultimate structural units of all these crystalline phases are TiO_6 octahedral with dissimilar lattice structure configurations [91,92].

The thermodynamic phase stability of nanocrystalline TiO_2 correlates with grain size. It was established for particles of similar size that rutile phase exhibits higher thermodynamical stability above 35 nm. Anatase, on the other hand, displays more stability for size below 11 nm [93]. For particles' size within the range 11-35 nm, brookite phase is the most stable. However, the synthesis of high purity single crystalline phase brookite is very rare in the literature [94]. Therefore, most practical studies on the ability of TiO_2 semiconductor materials to act as photocatalysts for the removal of EOPs are accomplished using anatase or mixed anatase/rutile phases.

There are several ways to produce TiO_2 nanoparticles and these include the sulphate or chloride processes. The sulphate process requires ilmenite ($FeTiO_3$) concentrate (40 to 60% TiO_2) as a base material, while the chloride route consists of converting ilmenite or other titanium-containing precursors to titanium tetrachloride ($TiCl_4$) *via* the reaction with elemental chlorine [95]. Both chloride and sulphate methodologies afford TiO_2 in the rutile crystalline form. However, the sulfate route can be manipulated to produce the anatase form. The vapor-phase hydrolysis of $TiCl_4$ at 360-550°C has been found to produced amorphous or anatase grains [96,97]. Hydrolysis of $TiCl_4$ at room temperature represents a common procedure for the synthesis of amorphous TiO_2 nanoparticles. The sol-gel preparation involves the hydrolysis of titanium alkoxides. This approach often yields anatase nanocrystals from the hydrolyzing titanium precursors [98,99]. Another approach is by chemical vapour deposition (CVD) technique, wherein the alkoxide is vaporized and subsequently decomposed on contact with a hot surface. The hydro- or solvothermal treatment of titanium precursors is classically carried out in an autoclave to yield anatase phase particles [100]. High temperature deposition or annealing (above 600 °C) frequently results in irreversible phase transition from anatase to rutile through Ti-O bonds rupture and rearrangement of octahedra TiO_6 from 4-edge sharing connectivity to 2-edge sharing and vertices connectivity [101–103].

This phase transformation is also associated with a reduction in the generated TiO_2 specific surface area.

Both rutile and anatase powders display bandgaps of 3.0 and 3.2 eV, respectively, thus falling into the UV region of the electromagnetic spectrum [104]. However, relative to rutile, TiO_2 anatase is considered to be suitable for application in photocatalysis owing to its enhanced charge carrier mobility and high amount of surface –OH groups [105]. Commercially available TiO_2 Degussa P25, which is regularly employed as a benchmark photocatalyst in light-induced oxidative degradation consists of anatase and rutile polymorphs in an approximate 3:1 ratio. Transmission electron microscopy (TEM) micrograph analysis of this material reveals agglomerates of anatase and rutile particles. When involved in photocatalytic reactions, these agglomerates are decomposed, and both phases are in contact with each other, thereby leading to a synergy effect [106]. Interfaces between both phases are further considered to improve the light-induced catalytic activity by minimising the possible charge carriers recombination. As a result, biphasic titanium dioxide possesses enhanced photo reactivity. It is also generally argued that the photocatalytic performance of anatase is associated with the shape and exposed facets [107].

Basically, three important low-index surfaces are displayed in TiO_2 crystalline structure and these include {001}, {100} and {101} as illustrated in Fig. 4 [108]. Nanosized anatase TiO_2 unveils better activity in ultraviolet (UV) irradiance. Under equilibrium or natural conditions, anatase TiO_2 crystal shows a tetragonal bipyramidal shape dominated by thermodynamically stable and less reactive {101} facets (Fig. 4a), according to the Wulff construction [109]. The adopted shape is concomitant with the surface energies of different facets. The Facets having high energies are set to grow faster under equilibrium or natural conditions. The surface energies of {101}, {100} and {001} are known to be 0.44, 0.53 and 0.90 J/m^2. These surface energies may be modified effectively through sorption of selected inorganic ions and/or organic molecules as capping agents for facets tailoring and morphology control [110,111]. Relatively to {101} and {100} facets, the {001} surfaces of anatase TiO_2 have been proven to demonstrate better catalytic efficiency for the photodegradation of organic contaminants [112]. Furthermore, recent development in anatase TiO_2 surface analysis using scanning tunnelling microscopy and DFT calculations techniques informed that band reduction for boosted photoactivity could also be effected using phase with titanium-terminated surface [113].

4. EOPs photocatalytic degradation over nanostructured TiO_2

4.1. TiO_2 anatase with {001}-facets exposed

The crystallinity, morphology and surface energy of nanostructured TiO_2 strongly influence its catalytic activity. The facet-dependent photo-assisted degradation of EOPs has been described across the literature. For example, Sayed et al. [114] described the degradation of bezafibrate under UV illumination and oxygen gas atmosphere using anatase TiO_2 with exposed {001} surfaces at a titanium sheet. This catalyst was obtained by the hydrothermal treatment (180 °C) of titanium foil in 0.03 M hydrofluoric acid (HF) and isopropanol, followed by calcinations of the resulting sheet at 600 °C. The Raman spectrum analysis of the as-synthesised TiO_2/Ti film unveiled 57% of reactive {001}-facets for the obtained single crystals. The apparent pseudo-first order rate constant for UV-assisted ($\lambda = 254$ nm) decomposition of bezafibrate (10 mg/L) by the $OH^•$ radicals attack was estimated to be 0.036 min^{-1}.

A mixture of isopropanol and HF serve as morphology controlling medium for the growth of single crystals anatase having a greater percentage of {001} surfaces exposed [115]. Fluoride ions adsorption by substitution of the surface –OH groups at {001}-facets during the growth of single crystals decreases their surface energy and consequently promotes the isotropic growth of 2D lateral size (Fig. 4b). However, although F^- ions are valuable as capping agent, the presence of fluorine atoms at the {001}-facets was found to reduce the photocatalytic efficiency of the grown nanoparticles [116]. In a separate study, this capping agent was removed on the TiO_2 anatase crystal surfaces by calcination (below 700 °C) [117]. In the same vein, Liao and co-workers [118] described a relatively superior catalytic activity of TiO_2 anatase nanocrystals film toward 4-chlorophenol after the removal of fluorine atoms on the exposed {001}-facets. Two films consisting of TiO_2 anatase single crystals were obtained by the electrochemical treatment of titanium metal to generate TiO_2 nanotubes, followed by heat application at 450 and 600 °C. The electrolyte was made up of an aqueous solution of ammonium fluoride and ethylene glycol. Relative to TiO_2 anatase single crystals film with surface fluorine atoms (product at 450 °C), the single crystals TiO_2 film with clean {001}-facets (product obtained at 600 °C) exhibited up to 2.5 times higher activity. Similarly, Sayed et al. also assessed the potentiality of TiO_2 anatase with resolved {001} facets at Ti films, obtained using varying concentrations (0.01-
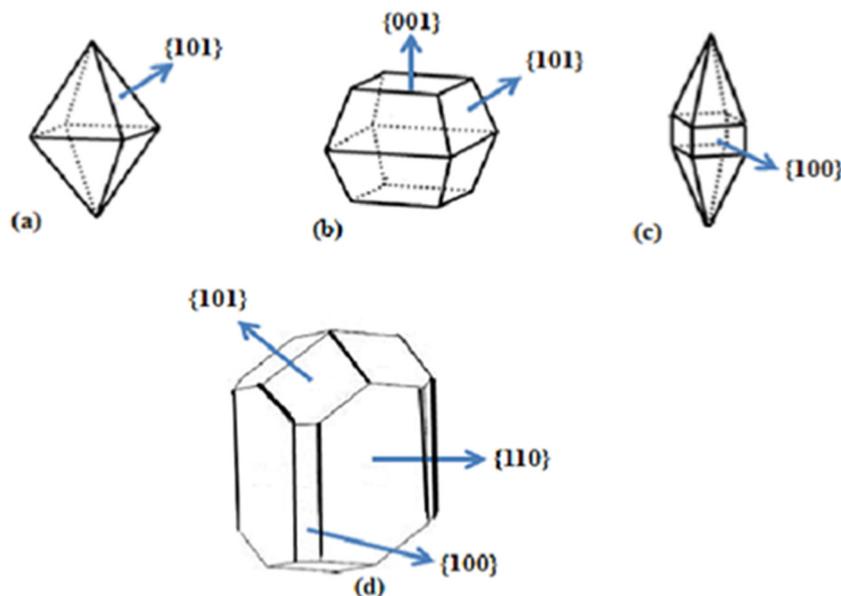

Fig. 4. Schematic illustration of anatase (a-c) and rutile (d) TiO_2 crystal shapes and exposed facets

0.04 M) of HF, for the degradation of antibacterial norfloxacin (10 mg/L) in aqueous solutions [119]. Interestingly, {001}-faceted film catalyst fabricated using 0.02 M HF displayed impressive photoactivity with rate constant of 0.0504 min^{-1}. The relatively higher efficiency of this photocatalyst was attributed to both an increase percentage of the exposed {001} facets (57%) and a reduce number of charge carriers recombination sites. Furthermore, based on the scavenger experiments, the authors argued that the photoexcited h^+ and e^- could gather at the {001} and {101} facets, respectively, for photocatalytic oxidation, and reduction reactions, as shown in Fig. 5.Degradation of norfloxacin occurred through attack by the generated $OH^{\bullet}$ radicals on the quinolone framework and piperazinyl ring as shown in Scheme 1. On the other hand, Fessi et al. [120] has recently demonstrated via UV photoelectron spectroscopy and time-resolved fluorescence spectroscopy techniques that the presence of fluorine at the surface of TiO_2 anatase induces the occurrence of intra bandgap with energy levels at around 1.3 eV. This material was found to exhibit a 2-fold higher photoactivity than the unamended TiO_2 anatase and Degussa P25for the decomposition of 1-methylnaphtalene contaminant in aqueous solution.

In addition, Zhang and co-workers [121] developed single crystals with 80% exposed {001} facets of TiO_2 for the treatment of synthetic water containing 4-chlorophenol under UV illumination. The photocatalyst was prepared by the microwave-assisted hydrothermal synthesis at 210 °C, using titanium tetrafluoride (TiF_4) precursor in the presence of 1-butyl-3-methylimidazolium tetrafluoroborate ([bmin][BF_4]) ionic liquid as the growth-controlling agent. The relatively higher percentage of {001}-facets was ascribed to the bulkier [BF_4]$^-$groups that could stabilize {001}-facet, more so than fluoride ions.

Although anatase phase of TiO_2 is considered as the most photoactive polymorph for catalytic degradation of organic pollutants, reports also suggest a relatively improved activity in biphasic TiO_2. Besides, TiO_2 anatase photocatalyst is only suitable for application in UV light-driven operation. Irradiation with relatively cheap visible light has been conceded as an ideal approach that could lower the costs associated with the photocatalytic water treatment technology, bearing in mind that UV irradiation only covers less than 5% of the solar spectral irradiance [74,122–124].

4.2. Mixed-phase TiO_2

The photocatalytic activity of mixed phases TiO_2 rutile-anatase for EOPs abatement has been observed to be relatively higher as compared to TiO_2 single-phase. To illustrate this difference in photoactivity, Apopei isolated anatase and rutile from TiO_2 mixed-phase Degussa P25 by dissolution in H_2O_2/NH_4OH solution, and subsequently evaluated their catalytic activity towards an EOP under UV lamp radiation [125]. Degussa P25 (200 mg/L) successfully decomposed (99%) 4-chlorophenol (10 mg/L) in 500 mL of an aqueous solution within 120 min of contact time. The separated anatase and rutile crystalline
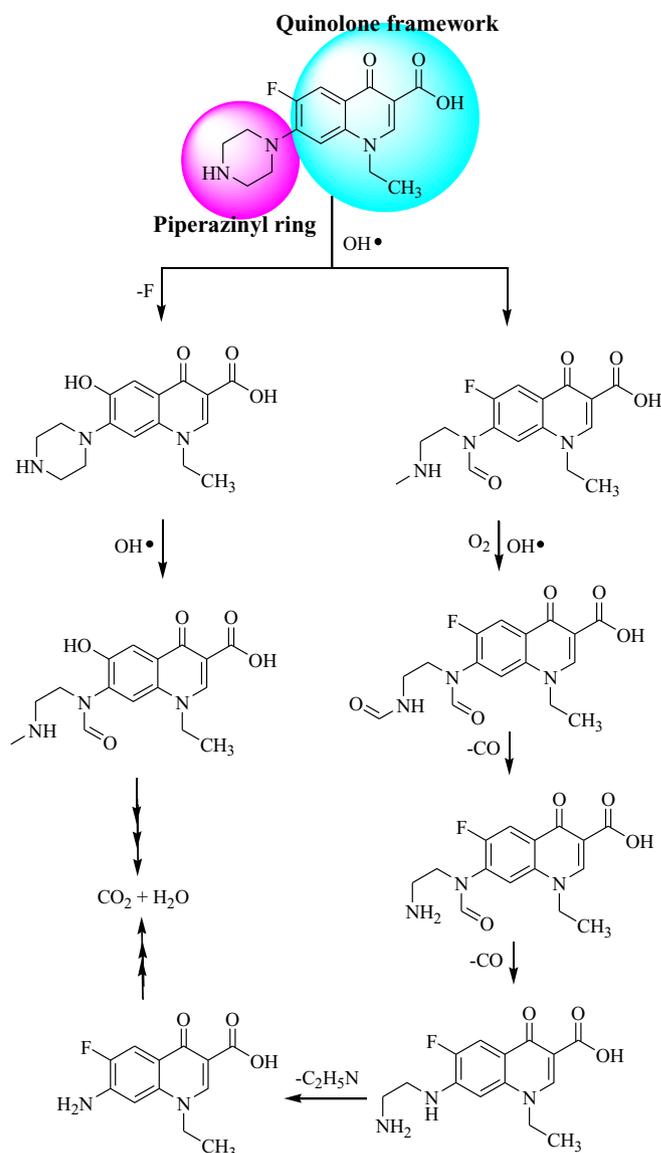
Scheme 1. Proposed pathway for the decomposition of norfloxacin using TiO_2 anatase with exposed {001} facets at Ti film.

phases, on the other hand, were found to display lower efficiencies with 85 and 50% of 4-chlorophenol oxidation, respectively, under similar reaction conditions. The notable photocatalytic performance of TiO_2 anatase-rutile combined phases is ascribed to the extended charge
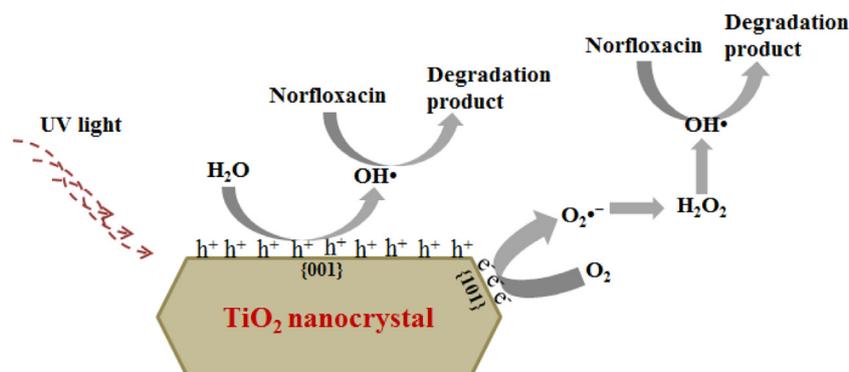
Fig. 5. Schematic illustration for the degradation of norfloxacin at a single crystal anatase with {001} facets exposed under UV irradiation and oxygen atmosphere [120]

carriers lifetime owing to a possible transfer at the phase junction. However, conflicting models for the favoured transfer mechanism are presented in the literature. According to the SEM micrographs of a bilayer-type TiO_2 anatase-rutile catalyst after photo-induced deposition of Ag particle, Kawahara and co-workers [126] anticipated that the charge separation took place via e$^-$ transfer from anatase CB to that of rutile as depicted in Fig. 6 (Model 1) [127,128]. However, based on the electron paramagnetic resonance (EPR) spectra analysis of Degussa P25, Hurum et al. argued that the charge separation resulted from the interfacial e$^-$ transfer from rutile CB to lower energy anatase lattice trapping sites as illustrated in Fig. 6 (Model 2) [129]. Lately, Shen group [130] suggested the movements of photoexited electrons from anatase CB and its trapping states to rutile CB at the phase junction, based on the anatase, rutile and mixed-phase transient mid-infrared (MIR) absorption spectra analysis. While anatase in the presence of methanol vapor ash$^+$ scavenger displayed transient MIR absorption under 355 nm laser pulse excitation due to the availability of photoexcited electrons, no absorption was observed on single-phase rutile sample. Moreover, a decrease in transient MIR absorption of TiO_2 mixed-phase with reduced amount of anatase phase was observed. These observations were in accordance with the model 1 (Fig. 6) of the charge separation in TiO_2 anatase-rutile mixed phases.

There are several reports on the use of TiO_2 mixed-phase for the removal of EOPs in aqueous environment. For example, Mohapatra and Nayak [131] reported the synthesis of TiO_2 nanocrystalline biphase (68% anatase and 32% rutile) via a thermal treatment (270 °C) of titanium tetraisopropoxide (TTIP) in oleic acid and calcination of the resultant precipitate at 450 °C. The XRD pattern of the samples after calcination at 400 °C and 600 °C revealed mainly anatase and rutile, respectively. The BET analysis of biphasic catalyst showed a specific surface area of 78 m^2/g and an apparent rate constant of 0.03 min^{-1} for the transformation of 2,4-dihydroxybenzoic acid (35 μM) in aqueous solution under UV irradiation. 2,4-Dihydroxybenzoic acid (DHBA) is often reported in wastewater generated in the olive processing industries [132]. It was presumed in this investigation that the UV-excited h$^+$ species initiated the decomposition of DHBA by oxidation to its radical cation; and O_2•$^-$ radicals were responsible for the formation of unstable molecules and ring opening (Scheme 2).

Recently, Wang et al. [133] utilized titanyl sulfate ($TiOSO_4$) and different amount of peroxide titanic acid in a hydrothermal process, to prepare mixed-TiO_2 phase powders with various anatase-to-rutile ratio (29 to 100% of anatase) and subsequently evaluated their photoreactivity towards phenol in aqueous solution. According to these authors, the ideal polymorph composition for the decomposition of phenol under a fluorescent lamp irradiation was 58.5 % anatase and 41.5% rutile. While Degussa P25 and pure TiO_2 anatase exhibited 90 and 85% of phenol degradation, respectively, and the model photocatalyst demonstrated 95% degradation after 12 h of visible light irradiation. Earlier, Su and co-workers [134] suggested the existence of synergetic effect between anatase and rutile which became highly pronounced with anatase percentage ranging from 40 to 80%. Alongside the fact that phase

junction has been established as an effective approach for the improvement of the TiO_2 photoactivity, numerous other approaches, including, metal and nonmetal doping, noble metal deposition and semiconductor coupling have also been valued [135].

4.3. Doped TiO_2 photocatalysts

Doping has been widely recognized as one of the key practices to engineer TiO_2 with reduced recombination of excited charge carriers (e$^-$/h$^+$) pair and improved photocatalytic activity. This technique allows for the modification of TiO_2 electrical features through the creation of defect states that results in reduced band gap energy [136]. Metal ions such as Ni^{2+}, Fe^{3+}, Co^{2+}, Al^{3+}, Sm^{3+} and Cu^{2+} have been used as dopants for the TiO_2 improved photodegradation of EOPs in aquatic media. For example, Blanco-Vega et al. [137] reported the synthesis of 0.5 and 1% Ni^{2+} doped TiO_2, by a microwave-assisted sol-gel procedure using TTIP precursor in the presence of a nickel salt, and their application for BPA degradation in visible light. As compared to pristine TiO_2 (Eg = 3.08 eV, Efficiency = 60%) and 0.5% Ni^{2+} doped TiO_2 (Eg = 2.75 eV, Efficiency = 83%), the 1% Ni^{2+} doped TiO_2 catalyst (1g/L) with a band gap energy of 2.72 eV exhibited 93% abatement of BPA (10 mg/L) after 120 min. Furthermore, this tuned TiO_2-based photocatalyst could also achieve 77% of BPA mineralization after 210 min exposure time. In a separate study, Wang and co-workers [138] described the synthesis of Fe^{3+} doped TiO_2 spherical-like particles at the polysulfone ultrafiltration membranes, and investigated their potential application in water pollution abatement. This was illustrated by discussing the BPA degradation at the prepared membrane photocatalysts and their self-cleaning capability. The as-described photocatalysts were obtained via the hydrothermal treatment of iron(III) nitrate and Degussa P25, followed by the phase inversion process with the membrane casting solution. The use of membrane catalyst (0.20 g) with Fe-TiO_2 mass ratio 20% resulted in 90.8% decomposition of BPA (10 mg/L in 250 mL) after 180 min exposure time in visible light irradiation with the 500 W Xenon lamp. The effectivity of this material was attributed to the Coulombic adsorption of BPA onto the polymer support and its decomposition by the Fe^{3+} doped TiO_2 nanoparticles. The visible light responsive ability of this catalyst relates to the narrow band gap that could be ascribed to the existence of d–d transitions of Fe(III) and the charge transfer transitions between interacting Fe(III) ions. The latter promote the occurrence of Fe(II) and Fe(VI) energy states across the band gap of TiO_2 [139,140]. During the Fe^{3+} doped TiO_2 photocatalytic activity, the Fe(III), Fe(II) and Fe(VI) ions are expected to serve as e$^-$ and h$^+$ trapping locations. Fig. 7 shows a plausible mechanism for the increased performance of Fe^{3+} doped TiO_2 catalyst in visible light irradiance.

Metal nanoparticles, with a lower Fermi level than the conduction band of semiconductors; also accumulate photogenerated e$^-$ after being deposited onto TiO_2, thus promoting the charge separation and an improved catalytic activity as shown in Fig. 8. Nevertheless, beyond the optimal metal loading, photocatalytic performance is reduced owing to the formation of e$^-$/h$^+$ recombination centers [141,142]. For
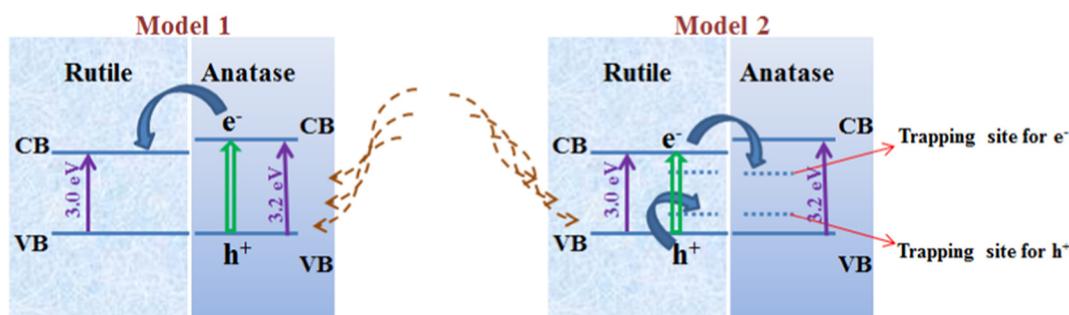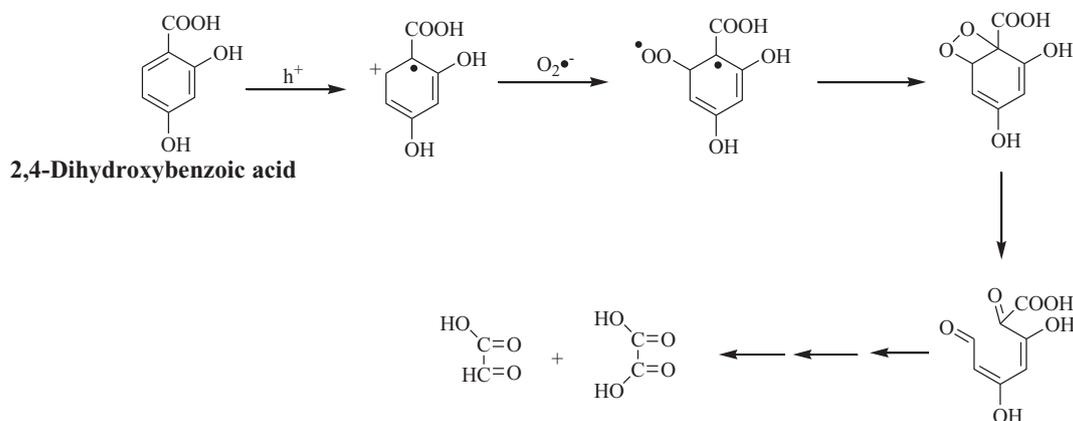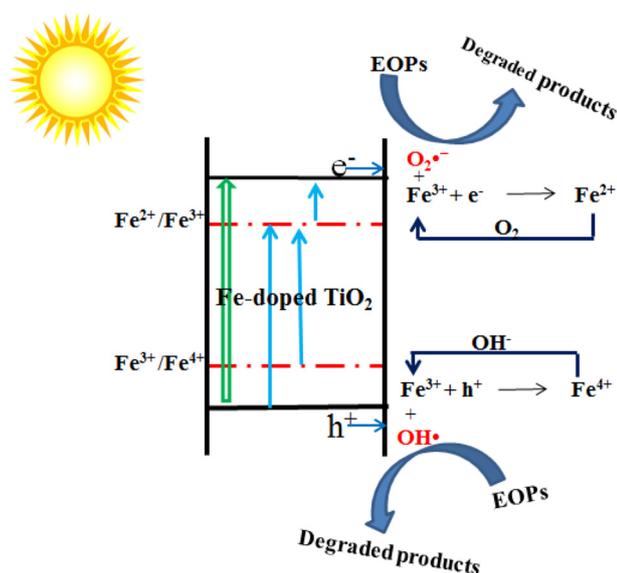

Fig. 6. Proposed model of the charge separation in TiO_2 anatase-rutile mixed
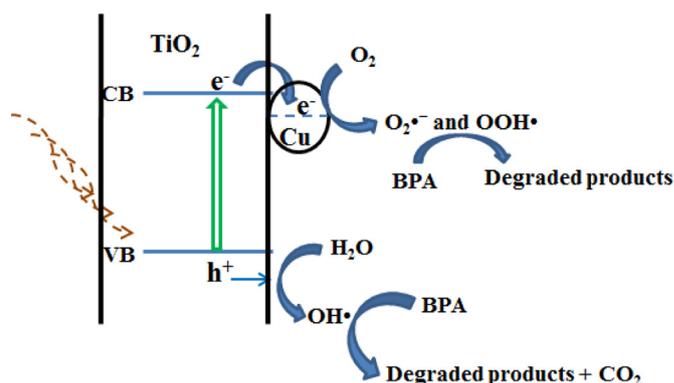
Scheme 2. Proposed mechanism for the decomposition of 2,4-dihydroxybenzoic acid using TiO_2 nanocrystalline mixed-phase.

Fig. 7. Proposed diagram for the improved photocatalytic activity of Fe^{3+} doped TiO_2 under visible light illumination

Fig. 8. Schematic diagram for the Cu-deposited TiO_2 improved photodegradation of EOPs.

example, 7% Cu deposited TiO_2 nanotubes, synthesized *via* a microwave-assisted sol-gel procedure using TTIP and copper(II) nitrate precursors, were found to show 3.8 and 6.6 times enhance degradation of BPA than Degussa P25 under UV and visible light illumination, respectively [143]. An increase in Cu loading from 7 to 20% led to a decrease (from 0.116 to 0.023 min^{-1}) in the rate constant for BPA photodecomposition. The chemical structures of the degradation intermediates were proposed based on the high-performance liquid chromatography-mass spectrometry data analysis and these are presented in Table 1. BPA degradation at Cu deposited TiO_2 under UV light irradiation was suggested to initiate oxidatively *via* 'OH radicals attack on one of the phenyl groups to give monohydroxylated BPA (**A**) [144]. The C-C bond cleavage between the isopropyl group and the phenyl moiety of BPA was found to generate compounds (**B**) and (**C**).Compounds (**D**) and (**E**) were formed *via* cleavage of electron rich aromatic ring by the attack of electrophilic 'OH radicals [145].

The anchoring of noble metals onto the surface or lattice layers of TiO_2 semiconductor has also been described as an important technique for the development of solar or visible light response catalyst. For example, Ag doped TiO_2 (25 mg), synthesized by Hlekelele and co-workers [146] using the deposition-precipitation strategy, has been reported to demonstrate 91% photocatalytic abatement of BPA (60 ppm) in 50 ml synthetic water under visible light irradiation. Comparative to virgin

TiO_2 and TiO_2/zeolite composite, the increased photocatalytic behaviour of Ag/TiO_2 was attributed to silver nanoparticles facility to harvest visible light through surface plasmon resonance (SPR) phenomenon. SPR is known to be the resonance coherent oscillation of e^- in the CB of a metal particle. This is persuaded by the electromagnetic field of an incident radiation [147]. Under this condition, the hot e^- can experience band transfer with the coupled semiconductor; leaving h^+ within the metal. The separated charge carriers initiate the redox reactions for EOPs decomposition [148,149]. Furthermore, this phenomenon could also induce the amplification of an internal electrical field, accountable for an increased light absorption cross-section and an improved separation of the charge carriers [148]. A different mechanism for the suppression of e^-/h^+ recombination, based on the higher work function of deposited noble metals has also been reported to ease the withdrawal of excited electrons from TiO_2 upon irradiation with UV light [142,150–152].

TiO_2 doping with non-metals such as phosphorus (P), sulfur (S), carbon (C), and nitrogen (N) is another strategy that has been established to produce photocatalyst with an improved activity under solar or visible light. This technique takes advantage of the possible electronic transition from the induced new electronic states above TiO_2 VB(2p or 3p orbitals of the dopant) to TiO_2 CB (3d orbitals of Ti). For instance, it was found that the degradation activity of nanosized N/F-codoped TiO_2 particles toward BPA was 3-fold higher than that of pristine TiO_2 [153]. The as-described photocatalyst was synthesized *via* the sol-gel method using EDTA and Zonyl® FS-300 fluorosurfactant as N and F sources. The BET and UV-visible spectroscopic analysis of the modified TiO_2 photocatalyst revealed a surface area of 136 m^2/g, an average particle size of 10.6 nm and a band gap of 2.87 eV. According to this report, the pronounced activity of this engineered TiO_2 photocatalyst was

Table 1

BPA degradation intermediates using Cu-TiO$_2$ nanorods under UV illumination.

m/z value	Proposed chemical structures	Names
244		2(Dihydroxyphenyl)-2-(4-hydroxyphenyl)propane (**A**)
134		4-Isopropenylphenol (**B**)
136		4-Hydroxyacetophenone (**C**)
208		3-(4-Hydroxy-phenyl)-3-methyl-2-oxo-butyric acid (**D**)
122		4-Hydroxybenzaldehyde (**E**)

attributed to N-doping (Fig. 9), a superior surface acidity due to F-doping and elevated total surface area. N-doping could take place either through the substitution of O atoms in the TiO$_2$ lattice or by occupying an interstitial position [154]. The doping effect of N/F created new defect states in the TiO$_2$ band gap, above its conduction band [155–157]. It has also been reported that doping TiO$_2$ with fluorine atom could improve the photocatalytic performance by decreasing the rate of e$^-$/h$^+$ pair recombination, following the creation of oxygen vacancies and Ti^{3+} surface state [158–160]. Table 2 summarises the selected investigations on photodegradation of EOPs by metal and non-metal doped-TiO$_2$ photocatalysts. Another modification that has been demonstrated to improve charge separation, lower the band gap energy, and lessen the rate of recombination is the use of coupled semiconductors.

It can be seen from Table 2 that the degradation efficiency of the pollutants and the reaction rate constants depend on several factors such as the synthesis protocol, nature of the dopants, concentration of the pollutants, surface area of the photocatalyst, band gap energy, and light source.

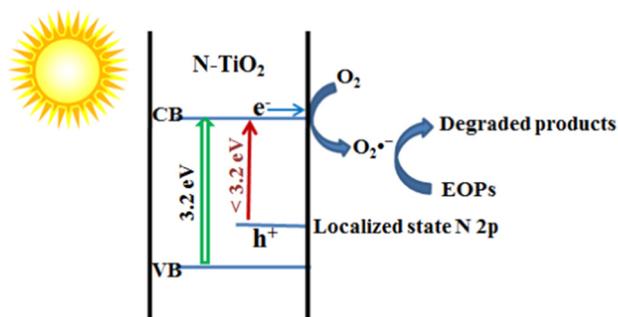*4.4. Heterogeneous photocatalysts consisting of TiO$_2$ and other materials*

The ability to obtain appropriate band gap energy by pairing TiO$_2$ with other materials having desirable visible light absorption potency is favourable for sunlight driven decomposition of EOPs in the aquatic environment. For example, Simsek et al. [161] described the ternary semiconducting rGO/TiO$_2$/ZnO heterojunction having a bandgap of 2.5 eV as a better photocatalyst for BPA, ibuprofen and flurbiprofen

Fig. 9. Origin of enhanced catalytic activity of N-doped TiO$_2$ under visible-light illumination.

decomposition under visible light illumination (400-800 nm). This hybrid photocatalyst was obtained by the hydrothermal process using graphite powder, F-doped TiO$_2$ film and zinc nitrate as the starting materials. Because of the inherent characteristics of graphene, including high electron mobility, large surface to volume ratio and superior chemical stability; the graphene-containing materials have attracted much interest in the development of photocatalysts with potential solar energy conversion ability [162,163]. The huge π-π network of graphene can serve to capture the photoexcited electrons, when associated to semiconductor such as TiO$_2$, thereby suppressing the charge recombination phenomenon [164]. In addition, through *d*-π interaction, graphene can contribute in narrowing the energy band gap of TiO$_2$/rGO-containing nanocomposites [165,166]. The construction of p-n heterojunction photocatalysts with direct interaction between n-type TiO$_2$ and p-type active semiconductors is also widely employed to achieve charge separation for EOPs degradation, based on the induced inner electric field at the interface [167–170]. To illustrate this statement, Sánchez-Rodríguez and co-workers [171] exploited the time resolved microwave conductivity measurements in p-n junction BiOCl/TiO$_2$ to argue that while excited-state holes in BiOCl migrate to TiO$_2$-VB, the electrons in TiO$_2$-CB could diffuse toward BiOCl-CB. This composite was synthesized by the sol-gel process with commercially available BiOCl and TTIP as the precursors. BiOCl/TiO$_2$ composite (1 g/L) achieved up to 46% decomposition of phenol (50 mg/L) after a contact time of 6 h under visible light irradiation. In a cognate study with p-type BiOI, Li et al. [170] used the photocurrent measurements of TiO$_2$, BiOI and BiOI/TiO$_2$ composite under visible light-on and -off cycles to expose the improved transfer and separation of the charge carriers within the heterojunction.

Other materials with potential light harvesting properties and ability to decrease the charge recombination, which have recently been reported for light-induced catalytic activity, are conducting polymers [172,173]. For example, polyaniline-capped TiO$_2$/ZnO, fabricated by the *in-situ* oxidative polymerization of aniline monomer in the presence of pre-synthesized TiO$_2$/ZnO composite, showed 97% mineralization of *p*-cresol under UV light irradiation for 6 h and a rate constant value of 0.26 min^{-1} [174]. Table 3 displays the reported studies for the removal of EOPs by TiO$_2$ coupled photocatalysts.

4.5. Contribution of TiO$_2$ photocatalyst in hybrid AOPs technologies

Combining two or more different AOPs [i.e. hybrid AOPs] has also attracted considerable interest owing to the amplified capability in

Table 2
Doped TiO_2 Photocatalyst for EOPs degradation

Material	Preparation method	EOP (concentration)	Catalyst dose	Light source	Irradiation time (min)	Efficiency	Rate constant (K)	Reference
Sm(III), N,P-doped TiO_2	Sol-solvothermal at 160 °C and calcination at 550 °C	4-Chlorophenol (20 mg /L)	0.4 g/L	Visible (500 W high-pressure Xenon lamp)	120	100%	2.83×10^{-2} min^{-1}	[199]
Cu (7%)-deposited TiO_2	Sol-gel and microwave procedure at 180 °C	BPA (10 mg/L)	1 g/L	Visible	180	100%	5.40×10^{-2} min^{-1}	[143]
C/N-doped TiO_2	Sol-solvothermal at 80 °C and calcination at 550 °C	Phenol (20 mg/L)	0.4 g/L	UV (330 W Mercury lamp)	150	87%	-	[200]
Cr(III) (0.04%)-doped TiO_2	Sol-gel, microwave procedure at 150 °C and calcination at 500 °C	4-Chloro-2-methylphenoxy-acetic acid (10 mg/L)	1 g/L	Visible (Spectro-line 450 nm)	240	100%	4.10×10^{-3} min^{-1}	[201]
N(1.0%)/ Cu(0.5%)-doped TiO_2 immobilized on rectorite	Sol-gel and calcination at 500°C	4-Chlorophenol (20 mg /L)	1 g /L	Visible (300 W Xe arc lamp)	180	-	9.36×10^{-2} h^{-1}	[202]
In(3%)/S(1%)-doped TiO_2 onto rGO	Ultrasonication and solvothermal treatment at 140 °C	Atrazine (20 mg/L)	1 g/L	Visible (300 W Tungsten-xenon lamp)	20	100%	24.8×10^{-2} min^{-1}	[203]
N-doped TiO_2	Pyrolysis	Phenol (500 ppm)	0.5 g/L	Visible	425	>30%	-	[204]
Fe(III)(0.5%)-doped TiO_2	Sol-gel	Nitrobenzene (2.5×10^{-4} mol/L)	-	Visible (mercury lamp)	240	88%	$1.48 \times 10^{4} s^{-1}$	[205]
F-TiO_2	Sol-gel, calcination at 400 °C and wet impregnation	1-Methylnaphthalene (10 mg/L)	1 g/L	UV (PLL lamp)	180	> 95%	_	[120]

terms of reducing the processing time and restraining the generation of toxic intermediates [175–177]. Despite the numerous studies linked to hybrid AOPs, only limited literatures information is available on the contribution of photocatalysis coupled with other AOPs in oxidation of EOPs or the mineralization of by-products. Indeed TiO_2 photocatalysis is the fundamental technique that has been coupled to other AOPs like sonochemistry, electrochemistry and plasmachemistry.

In the current review, combinations of the TiO_2 photocatalysis with other AOPs are also highlighted. The enhanced performance of the hybrid system as compared to the individual AOPs efficiency has been reported [178,179]. This reflects the existence of synergistic effects of the hybrid AOPs. Generally, such combined processes are found to enhance

the formation of $^{\bullet}OH$ radical, leading to higher degradation rates of the target pollutant and an increase in the mineralisation of intermediate by-products formed**. However, some harmful effects can also be observed during these coupling processes.

Among the AOPs technologies applied for wastewater treatment, more emphasis has also been shown to the decomposition of EOPs by ultrasonically generated (US/sonolysis) reactive oxygen species in aqueous media [180–183]. In sonolysis, the ultrasound-induced development and implosive collapse (cavitation) leads to the formation of $^{\bullet}OH$ radicals. This process is highly praised for its ability to equally degrade hydrophobic pollutants owing to the presence of $^{\bullet}OH$ radical within the bubbles and H_2O_2 oxidant at the interface gas/liquid

Table 3
TiO_2 coupled photocatalysts for EOPs degradation.

Material	Preparation method	EOP (concentration)	Catalyst dose	Light source	Irradiation time (min)	Efficiency	Rate constant	Reference
MoO_3/TiO_2	Hydrothermal treatment at 160 °C and calcination at 350 °C	Rhodamine B (10 mg/L)		UV (50 W Mercury lamp)	50	97%	0.079 min^{-1}	[206]
$TiO_2/WO_3/GO$	Hydrothermal treatment at 120 °C	BPA (20 mg/L)	2 mg/L	Sunlight	420	93%	-	[207]
Ag_2O/TiO_2 loaded on chitosan/ polypropylene film	Photodeposition	Ampicillin (20 mg/L)	-	Visible (150 W Tungsten-halogen Lamp)	180	100%	-	[208]
GO/TiO_2	Anodization and electrochemical Anodization	Perfluorooctanoic acid (0.12-2.42 mmol/L)	50-100 μg/L	UV	240	83%	0.34 h^{-1}	[209]
$rGO/TiO_2/ZnO$	Hydrothermal treatments	BPA (10 mg/L)	0.5 g/L	Visible	180	99%	5.28×10^{-2} min^{-1}	[161]
$Fe_3O_4/SiO_2/TiO_2/rGO$	Co-precipitation and calcination at 450 °C	2,4-Dinitrophenol (0.2 g/L)	40 mg/L	UV	30	88%	0.14 min^{-1}	[210]
$CdTe/TiO_2$	Hydrothermal treatment at 120 °C	Tetracycline (20 mg/L)	0.6 g/L	Visible (Halogen lamp)	30	78%	-	[211]
$FeNi_3/SiO_2/TiO_2$	Sol-gel	Tetracycline (10 mg/L)	5 mg/L	UV	200	100%	2.5×10^{-3} min^{-1}	[212]
Sepiolite/ $BiOCl/TiO_2$	Hydrolysis-precipitation and calcination at500 °C	Tetracycline (50 mg/L)	0.6 g/L	Visible (400 W Xenon lamp)	180	90%	4.37×10^{-3} min^{-1}	[213]
TiO_2 interjected medical talc	Hydrolysis-precipitation and calcination at 400 °C	2,4-Dichlorophenol (50 ppm)	2 g/L	UV	120	99.5%	-	[214]

[184–186]. However, the absolute mineralization of organic pollutants in sonolysis takes a longer period time. Hence, a combination of this process with other advanced remediation procedures has been attempted [187–189]. The heterogeneous TiO_2 photocatalysis is an efficient technique that allows for the decomposition of hydrophilic molecules since these display greater affinity with the polar catalyst surfaces. Consequently, a mixed sonolysis (US) and TiO_2 photocatalysis (Light+TiO_2) affords a technology that could alleviate the drawbacks encountered with the self processes and merge their advantages in a synergistic manner [190]. Moreover, an acoustic cavitation progression is capable of cleaning the photocatalysts surface, thereby invigorating the active sites. For combined processes, the synergistic effect can be assessed by determining the synergy index (Eq. 20). Value greater than 1 indicates a beneficial synergy between the separate techniques.

$$\text{Synergy Index} = \frac{K(US + Light + TiO2)}{K(US + TiO2) + K(Light + TiO2)} \qquad (20)$$

Jagannathan et al. [191] reported the degradation of paracetamol by sonophotocatalytic procedure using TiO_2 in the presence of ferric iron and H_2O_2 at 213 kHz ultrasound. This hybrid technique showed evidence of a higher efficiency than that of the separate sonolysis and TiO_2 photocatalysis procedures. The calculated rates of paracectamol decomposition for sonophotocatalysis using TiO_2 (1 g/L) was 4.02 μM. min^{-1}, while that of individual technology, photocatalysis and sonolysis, was evaluated at 3.02 and 0.83 μM.min^{-1}, respectively. The photocatalysis contribution was estimated to be around 75% in the hybrid system. According to these results, the synergistic index was evaluated to be 1.04, pinpointing a synergistic outcome for the sono-assisted photocatalytic procedure. The advanced degradation was ascribed to the development of more $^{\bullet}OH$ radicals owing to the visible light-activated Fe-aqua complex. It is worth noting that though sonolysis is able to eliminate the target pollutant, photocatalysis proves to be more efficient for achieving EOPs mineralization, making both processes complementary to each other. Similarly, a study on the BPA and interesting synergistic effect of the combined sonolysis-TiO_2 photocatalysis system, depending on the TiO_2 loading is also reported [192]. For example, while the use of 0.05 g/L of TiO_2 in the combined system led to 62% elimination of the dissolved organic carbon (DOC), 0.5 g/L loading of TiO_2 resulted in only 49% removal of DOC. On the other hand, using 1 g/L TiO_2, lesser DOC elimination was achieved (6 and 12%) by ultrasound and photocatalysis, exclusively. This suggests that synergistic effect also depends strongly on the loading of photocatalyst (TiO_2) through the influence of cavitational activity. The degradation of diclofenac by sonophotocatalysis has also been reported using a variety of photocatalysts, including, TiO_2, Ag-TiO_2 and Fe-ZnO [177,193]. A proposed mechanism for the improved EOP degradation in ultrasound-assisted TiO_2 photocatalysis was based on the continuous cleaning of the catalyst surface for the increased production of free hydroxyl radicals. Nevertheless, this technology has also been found to experience a damaging effect for the degradation of phosphate-bearing organic compounds [194]. The slow degradation resulted presumably from the adsorption of degraded phosphate ions at the TiO_2 surface, thereby competing with the targeted organic pollutant.

TiO_2 photocatalysis and Fenton joined process is based on the reaction between the Fe^{2+} ions and H_2O_2 molecules to generate the $HO^{\bullet}$/$HOO^{\bullet}$ radicals. TiO_2 photocatalysis is a permanent source of H_2O_2 which occurs at two levels on the surface of the irradiated semiconductor (VB and CB). Indeed on the VB, the positive hole (h^+) reacts with the molecules of H_2O and the hydroxide ions HO^- to form the radical $HO^{\bullet}$ which recombine preferentially into H_2O_2 than to react with an organic pollutant (Eq. 7 & 8). At the CB, the photogenerated electrons (e^-) are trapped by dissolved oxygen O_2 giving rise to the superoxide anion radical $O_2^{\bullet-}$, a precursor of the formation of H_2O_2. This results in the presence of a significant amount of H_2O_2 which will be unused in solution. However, the addition of Fe^{2+} to this solution could trigger the Fenton

reaction and even photoFenton (under UV radiation). The combined TiO_2 photocatalysis (UV/TiO_2) and Fenton (Fe^{2+}/H_2O_2) system could significantly increase the EOPs degradation by shortening the reaction time of the independent operations and the overall treatment cost. The synergetic effect of homogeneous and heterogeneous photocatalytic procedure could also be interesting to highlight. In this type of combination the most frequently admired source of radiation in the literature is sunlight, which seems suitable to trigger both the photo-Fenton reaction and the photocatalytic activation on the surface of TiO_2 and synergistically boosts $OH^{\bullet}$ production at neutral pH. For example, the solar/TiO_2/Fe^{2+}/H_2O_2 process was previously reported to degrade organic compounds occurring in hospital wastewater [195]. In that investigation the chemical oxygen demand (COD) measurement and biodegradability value were utilized to assess the effectiveness of the system. It was found that the increased hybrid process efficiency emanates from a decrease in the reaction time of COD removal and the cost of treatment. In fact, COD removal efficiency at the optimum conditions for the solar/TiO_2/H_2O_2, solar/Fe^{2+}/H_2O_2 and a combination of these two processes (solar/Fe^{2+}/TiO_2/H_2O_2) were 85%,94% and 99%, respectively after 4 hours of treatment. In addition, their respective rate constants were 0.253 h^{-1}, 0.274 h^{-1} and 0.771 h^{-1}, and the synergetic index for the joined processes was calculated to be 1.5. A similar study carried out by Selvabharathi et al. [196] also demonstrated the synergistic outcome and effectiveness of the integrated solar/Fe^{2+}/TiO_2/H_2O_2 system for the treatment of chemicals-containing tannery wastewater.

A combined TiO_2 photocatalysis and electrochemical procedure also known as photoelectrocatalysis (PEC) is a technique in which the electric current is employed to increase the photoactivity of the TiO_2 semiconductor in the presence of light. The principle is mainly based on the irradiation of a photoelectrode consisting of a deposit/film of TiO_2, thus avoiding the additional filtration step. The production mechanism of photogenerated species is similar to that of photocatalysis except for the fact that the supported catalyst acts as an anode on which the illumination is effected. Therefore, instead of witnessing the charge carriers recombination drawback, the induced electrons rather participates in the generation of superoxide radicals ($O_2^{\bullet-}$) in the presence of dissolved oxygen at the cathode, due to the imposed electric current. Accordingly, this process leads to the permanent availability of holes within the aqueous media and the formation of hydroxyl radicals. Remarkably, apart from the properties of TiO_2 photoanode, the effectiveness of this treatment technique also depends on the parameters like pH, voltage/intensity, inter-electrode distance, EOPs concentration, illumination intensity and concentration of the supporting electrolyte [197]. For example, Cheng et al. [198] described the use of reduced TiO_2 nanotube photoanode for the degradation of diclofenac at a voltage of 0.4 V using a standard three-electrode protocol under visible light illumination. It emerged that the degradation kinetics were faster in PEC comparative to simple TiO_2 light-reponsive catalytic activity. The total elimination of refractory diclofenac was accomplished after 8 h in PEC while the photocatalysis technique under similar conditions afforded complete organic pollutant degradation after 10 h. The scavenging assays clearly indicated that the hydroxyl radicals were responsible for the effective degradation process.

5. Critical assessment and conclusion

This review is to demonstrate that water pollution triggered by EOPs could be addressed using heterogeneous photocatalysis technique. TiO_2-containing catalysts appear to be among the most auspicious candidates for remarkable activity in UV, visible and sunlight irradiation. This overview highlights some of the key features of TiO_2 systems for photocatalytic degradation of EOPs. Research progress on the development of TiO_2 anatase phase that exposes high-energy {001} surfaces and their application in UV-light driven catalytic activity is valued. Through fluorination during TiO_2 synthesis, {001} faceted anatase TiO_2

crystals could be achieved. Discussion on the improved catalytic activity of mixed anatase/rutile TiO$_2$ semiconductors, owing to the plausible interfacial transfer of electrons, is brought about. Minimising the rate of recombination of charge carriers ($h^+ + e^-$) significantly enhances the photoactivity of TiO$_2$ catalyst. Modification of TiO$_2$ photocatalyst for EOPs decomposition as well as mineralisation under light illumination is systematically presented. Several approaches, including metal ions doping, non-metal doping, metal nanoparticles deposition and semiconductor coupling are also discoursed. Deposition of plasmonic metal nanoparticles, metal ions and non-metal doping could generate catalysts with sunlight harvesting potential for cost effective water treatment operations. Integrating other advanced oxidation techniques to TiO$_2$ photocatalysis could also afford systems with highly improved efficiency. TiO$_2$-containing photocatalysis and its early hybrid technologies have demonstrated a great prospective as eco-friendly and sustainable treatment procedures for the nearly complete abatement of EOPs in the industrial effluents and sewage. This technology can overcome the limitations of the conventional technologies in water treatment plants. Meanwhile, there is no denying that some major technical difficulties could hamper its commercialization. To foster the industrialization of TiO$_2$ photocatalysis and hybrid technologies, the conceptualization of TiO$_2$-based reactors for the efficient exploitation of sunlight radiation and post-recovery of the catalyst should be accentuated. Magnetic separation of the spent catalysts could provide an easy strategy for isolation, recovering, and reusability of the nanoengineered TiO$_2$-containing magnetic particles. To further improve the photocatalytic performance of these remarkable nanomaterials, facilitate the post-recovery process and ease the handling, their stabilization or immobilization onto various supports should be encouraged. It should also be stressed that research articles that evaluate the performance of TiO$_2$-based materials toward EOPs in sampled effluents are rare in the literature. Investigation of this nature should give vital information on the parameters that might affect the performance of TiO$_2$-based sunlight-reactors in photocatalysis or hybrid technologies.

The presence of EOPs in the aquatic environment may cause rising concerns to the ecosystem and human health, specially the ecotoxicity, endocrine disruption, and development of resistant bacteria. These hazards are entering into the aquatic environment through domestic, hospital, agricultural, and industrial effluents. Their accumulation in the surface water results from their continuous unregulated release and resistance to the mostly applied treatment procedures. Indeed, there is a general consensus among policy-makers that EOPs pollution needs to be addressed in a systematic and coherent manner. It would be possible to anticipate the risks following the use of these contaminants by using an early warning system able to play a role of the "watchdog"

All in all, diverse strategies for EOPs photocatalytic degradation using TiO$_2$ single phase (anatase), biphasic (anatase-rutile), doped, and paired with other materials have been reported as alternative methods to overcome the incapacity of many other treatment technologies to efficiently remove EOPs from wastewater. The development of tandem processes such as sonolysis-photocatalysis, Fenton-photocatalysis and electrochemical-photocatalysis systems using TiO$_2$ could reverse the adverse effects observed with the use of paired TiO$_2$ in photocatalysis, exclusively. Despite these advances, the minimization of wastewater generation and the possibility of their reuse after recycling remain an issue. This is due to the fact that EOPs oxidative degradation using TiO$_2$ photocatalysts should be applied to numerous types of effluents generated under different regional or national conditions. Hence, specific waste conditioning, and important information regarding cost, and benefits, as well as the scale-up of this degradation method are yet to be publicized. Considering the incidents that could emerge from the planets interconnected environments, awareness on the harmful effects of EOPs by scientific advisors should be consistently disclosed at fundamentally deep levels, many of which are opaque to the great mass of humanity.

Declaration of Competing Interest

None

References

[1] M. Gavrilescu, K. Demnerová, J. Aamand, S. Agathos, F. Fava, Emerging pollutants in the environment: present and future challenges in biomonitoring, ecological risks and bioremediation, New Biotechnol. 32 (2015) 147–156, https://doi.org/10.1016/j.nbt.2014.01.001.

[2] P. D'Odorico, J. Carr, C. Dalin, J. Dell'Angelo, M. Konar, F. Laio, L. Ridolfi, L. Rosa, S. Suweis, S. Tamea, M. Tuninetti, Global virtual water trade and the hydrological cycle: patterns,drivers, and socio-environmental impacts, Environ. Res. Lett. 14 (2019) 053001, https://doi.org/10.1088/1748-9326/ab05f4.

[3] UNESCO-IHP International Initiative on Water Quality (IIWQ), Emerging pollutants in wastewater reuse in developing countries, 2014-2018.

[4] M. La Farre, S. Pérez, L. Kantiani, D. Barceló, Fate and toxicity of emerging pollutants, their metabolites and transformation products in the aquatic environment, Trends Anal. Chem. 27 (2008) 991–1007, https://doi.org/10.1016/j.trac.2008.09.010.

[5] D.J. Lapworth, N. Baran, M.E. Stuart, R.S. Ward, Emerging organic contaminants in groundwater: A review of sources, fate and occurrence, Environ. Pollut. 163 (2012) 287–303, https://doi.org/10.1016/j.envpol.2011.12.034.

[6] B. Kasprzyk-Hordern, R.M. Dinsdale, A.J. Guwy, The removal of pharmaceuticals, personal care products, endocrine disruptors and illicit drugs during wastewater treatment and its impact on the quality of receiving waters, Water Res. 43 (2009) 363–380, https://doi.org/10.1016/j.watres.2008.10.047.

[7] B. Petrie, R. Barden, B. Kasprzyk-Hordern, A review on emerging contaminants in wastewaters and the environment: current knowledge, understudied areas and recommendations for future monitoring, Water Res. 72 (2015) 3–27, https://doi.org/10.1016/j.watres.2014.08.053.

[8] J. Wang, S. Wang, Removal of pharmaceuticals and personal care products (PPCPs) from wastewater: a review, J. Environ. Manag. 182 (2016) 620–640, https://doi.org/10.1016/j.jenvman.2016.07.049.

[9] R.J. Fussell, M. Garcia Lopez, D.N. Mortimer, S. Wright, M. Sehnalova, C.J. Sinclair, A. Fernandes, M. Sharman, Investigation into the occurrence in food of veterinary medicines, pharmaceuticals, and chemicals used in personal care products, J. Agric. Food Chem. 62 (2014) 3651–3659, https://doi.org/10.1021/jf4052418.

[10] C. Rimayi, D. Odusanya, J.M. Weiss, J. de Boer, L. Chimuka, Contaminants of emerging concern in the Hartbeespoort Dam catchment and the uMngeni River estuary 2016 pollution incident, South Africa, Sci. Total Environ. 627 (2016) 1008–1017, https://doi.org/10.1016/j.scitotenv.2018.01.263.

[11] R. Elibariki, M.M. Maguta, Status of pesticides pollution in Tanzania–A review, Chemosphere 178 (2017) 154–164, https://doi.org/10.1016/j.chemosphere.2017.03.036.

[12] W. Duan, F. Meng, H. Cui, Y. Lin, G. Wang, J. Wu, Ecotoxicity of phenol and cresols to aquatic organisms: A review, Ecotoxicol. Environ. Saf. 157 (2018) 441–456, https://doi.org/10.1016/j.ecoenv.2018.03.089.

[13] S. Son, K. Nam, H. Kim, M.C. Gye, I. Shin, Cytotoxicity measurement of Bisphenol A (BPA) and its substitutes using human keratinocytes, Environ. Res. 164 (2018) 655–659, https://doi.org/10.1016/j.envres.2018.03.043.

[14] Transparency Market Research, Bisphenol A Market for Polycarbonates, Epoxy Resins and Other Applications-global Industry Analysis, Aize, Share, Growth and Forecast, 2013 2013–2019.

[15] G.M. Klečka, C.A. Staples, K.E. Clark, N. van der Hoeven, D.E. Thomas, S.G. Hentges, Exposure analysis of bisphenol A in surface water systems in North America and Europe, Environ. Sci. Technol. 43 (2009) 6145–6150, https://doi.org/10.1021/es900598e.

[16] A. Schecter, N. Malik, D. Haffner, S. Smith, T.R. Harris, O. Paepke, L. Birnbaum, Bisphenol a (BPA) in US food, Environ. Sci. Technol. 44 (2010) 9425–9430, https://doi.org/10.1021/es102785d.

[17] S. Gaw, K.V. Thomas, T.H. Hutchinson, Sources, impacts and trends of pharmaceuticals in the marine and coastal environment, Philos. Trans. R. Soc. B 369 (2014) 20130572, https://doi.org/10.1098/rstb.2013.0572.

[18] J. Im, F.E. Löffler, Fate of bisphenol A in terrestrial and aquatic environments, Environ. Sci. Technol. 50 (2016) 8403–8416, https://doi.org/10.1021/acs.est.6b00877.

[19] T. Colborn, F.S. VomSaal, A.M. Soto, Developmental effects of endocrine-disrupting chemicals in wildlife and humans, Environ. Health Perspect. 101 (1993) 378–384, https://doi.org/10.1289/ehp.93101378.

[20] C.A. Richter, L.S. Birnbaum, F. Farabollini, R.R. Newbold, B.S. Rubin, C.E. Talsness, J.G. Vandenbergh, D.R. Walser-Kuntz, F.S. Vomsaal, In vivo effects of bisphenol A in laboratory rodent studies, Reprod. Toxicol. 24 (2007) 199–224, https://doi.org/10.1016/j.reprotox.2007.06.004.

[21] I. Buka, A. Osornio-Vargas, R. Walker, Canada declares bisphenol A a 'dangerous substance': Questioning the safety of plastics, Paediatr. Child Health 14 (2009) 11–13.

[22] Y. Zhou, Z. Wang, M. Xia, S. Zhuang, X. Gong, J. Pan, C. Li, R. Fan, Q. Pang, S. Lu, Neurotoxicity of low bisphenol A (BPA) exposure for young male mice: Implications for children exposed to environmental levels of BPA, Environ. Pollut. 229 (2017) 40–48, https://doi.org/10.1016/j.envpol.2017.05.043.

[23] J.-S. Park, M.T. Brown, T. Han, Phenol toxicity to the aquatic macrophyte Lemna paucicostata, Aquat. Toxicol. 106-107 (2012) 182–188, https://doi.org/10.1016/j.aquatox.2011.10.004.

[24] Y. Yang, W. Song, H. Lin, W. Wang, L. Du, W. Xing, Antibiotics and antibiotic resistance genes in global lakes: A review and meta-analysis, Environ. Int. 116 (2018) 60–73, https://doi.org/10.1016/j.envint.2018.04.011.

[25] Y. Liu, M. Junaid, Y. Wang, Y.M. Tang, W.P. Bian, W.X. Xiong, H.Y. Huang, C.D. Chen, D.S. Pei, New toxicogenetic insights and ranking of the selected pharmaceuticals belong to the three different classes: a toxicity estimation to confirmation approach, Aquat. Toxicol. 201 (2018) 151–161, https://doi.org/10.1016/j.aquatox.2018.06.008.

[26] J. Ory, G. Bricheux, A. Togola, J.L. Bonnet, F. Donnadieu-Bernard, L. Nakusi, C. Forestier, O. Traore, Ciprofloxacin residue and antibiotic-resistant biofilm bacteria in hospital effluent, Environ. Pollut. 214 (2016) 635–645, https://doi.org/10.1016/j.envpol.2016.04.033.

[27] A.D. Lemly, Evaluation of the hazard quotient method for risk assessment of selenium, Ecotoxicol. Environ.Saf. 35 (1996) 156–162, https://doi.org/10.1006/eesa.1996.0095.

[28] T. Brodin, J. Fick, M. Jonsson, J. Klaminder, Dilute concentrations of a psychiatric drug alter behavior of fish from natural populations, Science 339 (2013) 814–815, https://doi.org/10.1126/science.1226850.

[29] B.K. González-Pérez, S.S. Sarma, S. Nandini, Effects of selected pharmaceuticals (ibuprofen and amoxicillin) on the demography of Brachionuscalyciflorus and Brachionushavanaensis (Rotifera), Egypt. J. Aquat. Res. 42 (2016) 341–347, https://doi.org/10.1016/j.ejar.2016.09.003.

[30] J. Zhang, J. Zhang, R. Liu, J. Gan, J. Liu, W. Liu, Endocrine-disrupting effects of pesticides through interference with human glucocorticoid receptor, Environ. Sci. Technol. 50 (2016) 435–443, https://doi.org/10.1021/acs.est.5b03731.

[31] R.M. Guimarães, C.I.R.F. Asmus, A. Meyer, DDT reintroduction for malaria control: the cost-benefit debate for public health, Cad. Saúde Pública 23 (2007) 2835–2844.

[32] M. Beato, P. Herrlich, G. Schütz, Steroid hormone receptors: many actors in search of a plot, Cell 83 (1995) 851–857, https://doi.org/10.1016/0092-8674(95)90201-5.

[33] P. Hakimi, M.T. Johnson, J. Yang, D.F. Lepage, R.A. Conlon, S.C. Kalhan, L. Reshef, S.M. Tilghman, R.W. Hanson, Phosphoenolpyruvatecarboxykinase and the critical role of cataplerosis in the control of hepatic metabolism, Nutr. Metab. 2 (2005) 33, https://doi.org/10.1186/1743-7075-2-33.

[34] J.D. McKinney, A. Richard, C. Waller, M.C. Newman, F. Gerberick, The practice of structure activity relationships (SAR) in toxicology, Toxicol. Sci. 56 (2000) 8–17.

[35] A. Khare, P. Jadhao, S. Paliya, K. Kumari, Toxicity and structural activity relationship of persistent organic pollutants, in: G. Baskar, K.S. Kumar, K. Tamilarasan (Eds.), Frontiers in enzyme inhibition, 1, 2020, pp. 174–203, https://doi.org/10.2174/9789811460821120010012.

[36] D.J. De Ridder, J.Q. Verberk, S.G. Heijman, G.L. Amy, J.C. Van Dijk, Zeolites for nitrosamine and pharmaceutical removal from demineralised and surface water: mechanisms and efficacy, Sep. Purif. Technol. 89 (2012) 71–77, https://doi.org/10.1016/j.seppur.2012.01.025.

[37] M.J. Ahmed, Adsorption of non-steroidal anti-inflammatory drugs from aqueous solution using activated carbons, J. Environ. Manag. 190 (2017) 274–282, https://doi.org/10.1016/j.jenvman.2016.12.073.

[38] R. Yendluri, D.P. Otto, M.M. De Villiers, V. Vinokurov, Y.M. Lvov, Application of halloysite clay nanotubes as a pharmaceutical excipient, Int. J. Pharm. 521 (2017) 267–273, https://doi.org/10.1016/j.ijpharm.2017.02.055.

[39] E.F. Lessa, M.L. Nunes, A.R. Fajardo, Chitosan/waste coffee-grounds composite: An efficient and eco-friendly adsorbent for removal of pharmaceutical contaminants from water, Carbohydr. Polym. 189 (2018) 257–266, https://doi.org/10.1016/j.carbpol.2018.02.018.

[40] Z. Jin, X. Wang, Y. Sun, Y. Ai, X. Wang, Adsorption of 4-n-nonylphenol and bisphenol-A on magnetic reduced graphene oxides: a combined experimental and theoretical studies, Environ. Sci. Technol. 49 (2015) 9168–9175, https://doi.org/10.1021/acs.est.5b02022.

[41] I. Bautista-Toledo, M.A. Ferro-Garcia, J. Rivera-Utrilla, C. Moreno-Castilla, F.J. Vegas Fernández, Bisphenol A removal from water by activated carbon. Effects of carbon characteristics and solution chemistry, Environ. Sci. Technol. 39 (2005) 6246–6250, https://doi.org/10.1021/es0481169.

[42] J.R. Koduru, L.P. Lingamdinne, J. Singh, K.H. Choo, Effective removal of bisphenol A (BPA) from water using a goethite/activated carbon composite, Process. Saf. Environ. Prot. 103 (2016) 87–96, https://doi.org/10.1016/j.psep.2016.06.038.

[43] R. Das, V.S. Sypu, H.K. Paumo, M. Bhaumik, V. Maharaj, A. Maity, Silver decorated magnetic nanocomposite (Fe₃O₄@PPy-MAA/Ag) as highly active catalyst towards reduction of 4-nitrophenol and toxic organic dyes, Appl. Catal. B 244 (2019) 546–558, https://doi.org/10.1016/j.apcatb.2018.11.073.

[44] M. Chigondo, H.K. Paumo, M. Bhaumik, K. Pillay, A. Maity, Hydrous CeO₂-Fe₃O₄ decorated polyanilinefibersnanocomposite for effective defluoridation of drinking water, J. Colloid Interface Sci. 532 (2018) 500–516, https://doi.org/10.1016/j.jcis.2018.07.134.

[45] M. Chigondo, H.K. Paumo, M. Bhaumik, K. Pillay, A. Maity, Magnetic argininefunctionalized polypyrrole with improved and selective chromium(VI) ions removal from water, J. Mol. Liq. 275 (2019) 778–791, https://doi.org/10.1016/j.molliq.2018.11.032.

[46] M. Zielińska, K. Bułkowska, A. Cydzik-Kwiatkowska, K. Bernat, I. Wojnowska-Baryła, Removal of bisphenol A (BPA) from biologically treated wastewater by microfiltration and nanofiltration, Int. J. Environ. Sci. Technol. 13 (2016) 2239–2248, https://doi.org/10.1007/s13762-016-1056-6.

[47] X. Jin, J. Shan, C. Wang, J. Wei, C.Y. Tang, Rejection of pharmaceuticals by forward osmosis membranes, J. Hazard. Mater. 227 (2012) 55–61, https://doi.org/10.1016/j.jhazmat.2012.04.077.

[48] Y. Cui, X.Y. Liu, T.S. Chung, M. Weber, C. Staudt, C. Maletzko, Removal of organic micro-pollutants (phenol, aniline and nitrobenzene) via forward osmosis (FO)

[49] process: evaluation of FO as an alternative method to reverse osmosis (RO), Water Res. 91 (2016) 104–114, https://doi.org/10.1016/j.watres.2016.01.001.

[49] Q. Yang, J. Lei, D.D. Sun, D. Chen, Forward osmosis membranes for water reclamation, Sep. Purif. Rev. 45 (2016) 93–107, https://doi.org/10.1080/15422119.2014.973506.

[50] M. Martins, S. Sanches, I.A. Pereira, Anaerobic biodegradation of pharmaceutical compounds: new insights into the pharmaceutical-degrading bacteria, J. Hazard. Mater. 357 (2018) 289–297, https://doi.org/10.1016/j.jhazmat.2018.06.001.

[51] B.E. Taştan, G. Dönmez, Biodegradation of pesticide triclosan by A. versicolor in simulated wastewater and semi-synthetic media, Pestic. Biochem. Physiol. 118 (2015) 33–37, https://doi.org/10.1016/j.pestbp.2014.11.002.

[52] A. Pariatamby, Y.L. Kee, Persistent organic pollutants management and remediation, Procedia Environ. Sci. 31 (2016) 842–848, https://doi.org/10.1016/j.proenv.2016.02.093.

[53] L. Sailo, D. Tiwari, S.M. Lee, Degradation of some micro-pollutants from aqueous solutions using ferrate (VI): Physico-chemical studies, Sep. Sci. Technol. 52 (2017) 2756–2766, https://doi.org/10.1080/01496395.2017.1374976.

[54] M.J. Quero-Pastor, M.C. Garrido-Perez, A. Acevedo, J.M. Quiroga, Ozonation of ibuprofen: a degradation and toxicity study, Sci. Total Environ. 466 (2014) 957–964, https://doi.org/10.1016/j.scitotenv.2013.07.067.

[55] U. Von Gunten, Ozonation of drinking water: Part I. Oxidation kinetics and product formation, Water Res. 37 (2003) 1443–1467, https://doi.org/10.1016/S0043-1354(02)00457-8.

[56] D. Gardoni, A. Vailati, R. Canziani, Decay of ozone in water: a review, Ozone Sci. Eng. 34 (2012) 233–242, https://doi.org/10.1080/01919512.2012.686354.

[57] W. Yao, S.W. Rehman, H. Wang, H. Yang, G. Yu, Y. Wang, Pilot-scale evaluation of micropollutant abatements by conventional ozonation, UV/O₃, and an electroperoxone process, Water Res. 138 (2018) 106–117, https://doi.org/10.1016/j.watres.2018.03.044.

[58] C. Afonso-Olivares, C. Fernández-Rodríguez, R.J. Ojeda-González, Z. Sosa-Ferrera, J.J. Santana-Rodríguez, J.D. Rodríguez, Estimation of kinetic parameters and UV doses necessary to remove twenty-three pharmaceuticals from pre-treated urban wastewater by UV/H₂O₂, J. Photochem. Photobiol. A 329 (2016) 130–138, https://doi.org/10.1016/j.jphotochem.2016.06.018.

[59] Y. Ku, W.J. Su, Y.S. Shen, Decomposition kinetics of ozone in aqueous solution, Ind. Eng. Chem. Res. 35 (1996) 3369–3374, https://doi.org/10.1021/ie9503959.

[60] L.V. Santos, A.M. Meireles, L.C. Lange, Degradation of antibiotics norfloxacin by Fenton, UV and UV/H₂O₂, J. Environ. Manag. 154 (2015) 8–12, https://doi.org/10.1016/j.jenvman.2015.02.021.

[61] E. Neyens, J. Baeyens, A review of classic Fenton's peroxidation as anadvanced oxidation technique, J. Hazard. Mater. 98 (2003) 33–50, https://doi.org/10.1016/S0304-3894(02)00282-0.

[62] L. Soler, V. Magdanz, V.M. Fomin, S. Sanchez, O.G. Schmidt, Self-propelled micromotors for cleaning polluted water, ACS Nano 7 (2013) 9611–9620, https://doi.org/10.1021/nn405075d.

[63] A.D. Bokare, W. Choi, Review of iron-free Fenton-like systems for activating H₂O₂ in advanced oxidation processes, J. Hazard. Mater. 275 (2014) 121–135, https://doi.org/10.1016/j.jhazmat.2014.04.054.

[64] B.H. Diya'uddeen, A.A.R. Abdul, W.M.A.W. Daud, On the limitation of Fenton oxidation operational parameters: a review, Int. J. Chem. React. Eng. 10 (2012)https://doi.org/10.1515/1542-6580.2913.

[65] A. Babuponnusami, K. Muthukumar, A review on Fenton and improvements to the Fenton process for wastewater treatment, J. Environ. Chem. Eng. 2 (2014) 557–572, https://doi.org/10.1016/j.jece.2013.10.011.

[66] J. Lee, U. von Gunten, J.-H. Kim, Persulfate-based advanced oxidation: Critical assessment of opportunities and roadblocks, Environ. Sci. Technol. 54 (2020) 3064–3081, https://doi.org/10.1021/acs.est.9b07082.

[67] S. Guerra-Rodríguez, E. Rodríguez, D.N. Singh, J. Rodríguez-Chueca, Assessment of sulfate radical-based advanced oxidation processes for water and wastewater treatment: A review, Water 10 (2018) 1828, https://doi.org/10.3390/w10121828.

[68] A.O. Ibhadon, P. Fitzpatrick, Heterogeneous photocatalysis: recent advances and applications, Catalysts 3 (2013) 189–218, https://doi.org/10.3390/catal3010189.

[69] H.K. Paumo, R. Das, M. Bhaumik, A. Maity, Visible-light-responsive nanostructured materials for photocatalytic degradation of persistent organic pollutants in water, in: M. Naushad, S. Rajendran, E. Lichtfouse (Eds.), Green methods for wastewater treatment, Environmental chemistry for a sustainable world, 35, Springer, Cham, 2020https://doi.org/10.1007/978-3-030-16427-0_1.

[70] M. Canle, M.I. Pérez, J.A. Santaballa, Photocatalyzed degradation/abatement of endocrine disruptors, Curr. Opin. Green Sustain. Chem. 6 (2017) 101–138, https://doi.org/10.1016/j.cogsc.2017.06.008.

[71] K.V. Kumar, K. Porkodi, Comments on "Photocatalytic properties of TiO₂ modified with platinum and silver nanoparticles in the degradation of oxalic acid in aqueous solution" Langmuir Hinshelwood kinetics-A theoretical study, Appl. Catal. B 79 (2008) 108–109, https://doi.org/10.1016/j.apcatb.2007.09.041.

[72] A. Malathi, J. Madhavan, M. Ashokkumar, P. Arunachalam, A review on BiVO₄photocatalyst: activity enhancement methods for solar photocatalytic applications, Appl. Catal. A 555 (2018) 47–74, https://doi.org/10.1016/j.apcata.2018.02.010.

[73] S.N. Habisreutinger, L. Schmidt-Mende, J.K. Stolarczyk, Photocatalytic reduction of CO₂ on TiO₂ and other semiconductors, Angew. Chem. Int. Ed. 52 (2013) 7372–7408, https://doi.org/10.1002/anie.201207199.

[74] S. Dong, J. Feng, M. Fan, Y. Pi, L. Hu, X. Han, M. Liu, J. Sun, J. Sun, Recent developments in heterogeneous photocatalytic water treatment using visible light-responsive photocatalysts: a review, RSC Adv. 5 (2015) 14610–14630, https://doi.org/10.1039/c4ra13734e.

[75] M.R. Khaki, M.S. Shafeeyan, A.A. Raman, W.M. Daud, Application of doped photocatalysts for organic pollutant degradation-A review, J. Environ. Manag. 198 (2017) 78–94, https://doi.org/10.1016/j.jenvman.2017.04.099.

[76] M.A. Henderson, A surface science perspective on TiO$_2$photocatalysis, Surf. Sci. Rep. 66 (2011) 185–297, https://doi.org/10.1016/j.surfrep.2011.01.001.

[77] A. Fujishima, X. Zhang, D.A. Tryk, TiO$_2$photocatalysis and related surface phenomena, Surf. Sci. Rep. 63 (2008) 515–582, https://doi.org/10.1016/j.surfrep.2008.10.001.

[78] S. Wang, L. Pan, J.J. Song, W. Mi, J.J. Zou, L. Wang, X. Zhang, Titanium-defected undopedanatase TiO$_2$ with p-type conductivity, room-temperature ferromagnetism, and remarkable photocatalytic performance, J. Am. Chem. Soc. 137 (2015) 2975–2983, https://doi.org/10.1021/ja512047k.

[79] O. Bechambi, S. Sayadi, W. Najjar, Photocatalytic degradation of bisphenol A in the presence of C-doped ZnO: effect of operational parameters and photodegradation mechanism, J. Ind. Eng. Chem. 32 (2015) 201–210, https://doi.org/10.1016/j.jiec.2015.08.017.

[80] M.G. Alalm, S. Ookawara, D. Fukushi, A. Sato, A. Tawfik, Improved WO$_3$photocatalytic efficiency using ZrO$_2$ and Ru for the degradation of carbofuran and ampicillin, J. Hazard. Mater. 302 (2016) 225–231, https://doi.org/10.1016/j.jhazmat.2015.10.002.

[81] J. Wen, C. Ma, P. Huo, X. Liu, M. Wei, Y. Liu, X. Yao, Z. Ma, Y. Yan, Constructionof vesicle CdSenano-semiconductors photocatalysts with improved photocatalytic activity: Enhanced photo induced carriers separation efficiency and mechanism insight, J. Environ. Sci. 60 (2017) 98–107, https://doi.org/10.1016/j.jes.2016.12.023.

[82] J. Bai, Y. Li, P. Jin, J. Wang, L. Liu, Facile preparation 3D ZnSnanospheres-reduced graphene oxide composites for enhanced photodegradation of norfloxacin, J. Alloys Compd. 729 (2017) 809–815, https://doi.org/10.1016/j.jallcom.2017.07.057.

[83] S. Begum, M. Ahmaruzzaman, Biogenic synthesis of SnO$_2$/activated carbon nanocomposite and its application as photocatalyst in the degradation of naproxen, Appl. Surf. Sci. 449 (2018) 780–789, https://doi.org/10.1016/j.apsusc.2018.02.069.

[84] X. Xie, K. Kretschmer, G. Wang, Advances in graphene-based semiconductor photocatalysts for solar energy conversion: fundamentals and materials engineering, Nanoscale 7 (2015) 13278–13292, https://doi.org/10.1039/c5nr03338a.

[85] X. Hu, X. Hu, Q. Peng, L. Zhou, X. Tan, L. Jiang, C. Tang, H. Wang, S. Liu,Y. Wang, Z. Ning, Mechanisms underlying the photocatalytic degradation pathway of ciprofloxacin with heterogeneous TiO$_2$, Chem. Eng. J. 380 (2020) 122366. doi: https://doi.org/10.1016/j.cej.2019.122366

[86] V. Srivastava, D. Gusain, Y.C. Sharma, Critical review on the toxicity of some widely used engineered nanoparticles, Ind. Eng. Chem. Res. 54 (2015) 6209–6233, https://doi.org/10.1021/acs.iecr.5b01610.

[87] S.N. Frank, A.J. Bard, Semiconductor electrodes. 12. Photoassisted oxidations and photoelectrosynthesis at polycrystalline titanium dioxide electrodes, J. Am. Chem. Soc. 99 (1997) 4667–4675, https://doi.org/10.1021/ja00456a024.

[88] O. Carp, C.L. Huisman, A. Reller, Photoinduced reactivity of titanium dioxide, Prog. Solid State Chem. 32 (2004) 33–177, https://doi.org/10.1016/j.progsolidstchem.2004.08.001.

[89] X. Chen, C. Burda, The electronic origin of the visible-light absorption properties of C-, N-and S-doped TiO$_2$nanomaterials, J. Am. Chem. Soc. 130 (2008) 5018–5019, https://doi.org/10.1021/ja711023z.

[90] B.J. Morgan, G.W. Watson, Intrinsic n-type defect formation in TiO$_2$: a comparison of rutile and anatase from GGA+U calculations, J. Phys. Chem. C 114 (2010) 2321–2328, https://doi.org/10.1021/jp9088047.

[91] N.H. Vu, H.V. Le, T.M. Cao, V.V. Pham, H.M. Le, D. Nguyen-Manh, Anatase–rutile phase transformation of titanium dioxide bulk material: a DFT + U approach, J. Phys. Condens. Matter 24 (2012) 405501, https://doi.org/10.1088/0953-8984/24/40/405501.

[92] S. Bagheri, Z.A. Hir, A.T. Yousefi, S.B. Hamid, Progress on mesoporous titanium dioxide: synthesis, modification and applications, Microporous Mesoporous Mater. 218 (2015) 206–222, https://doi.org/10.1016/j.micromeso.2015.05.028.

[93] H. Zhang, J.F. Banfield, Understanding polymorphic phase transformation behavior during growth of nanocrystalline aggregates: insights from TiO$_2$, J. Phys. Chem. B 104 (2000) 3481–3487, https://doi.org/10.1021/jp000499j.

[94] W.S. Koe, J.W. Lee, W.C. Chong, Y.L. Pang, L.C. Sim, An overview of photocatalytic degradation: photocatalysts, mechanisms, and development of photocatalytic membrane, Environ. Sci. Pollut. Res. 27 (2020) 2522–2565, https://doi.org/10.1007/s11356-019-07193-5.

[95] H. Bao, H. Zhang, G. Liu, Y. Li, W. Cai, Nanoscaled amorphous TiO$_2$ hollow spheres: TiCl$_4$ liquid droplet-based hydrolysis fabrication and strong hollow structureenhanced surface-enhanced Raman scattering effects, Langmuir 33 (2017) 5430–5438, https://doi.org/10.1021/acs.langmuir.7b00298.

[96] D. Li, H. Haneda, N.K. Labhsetwar, S. Hishita, N. Ohashi, Visible-light-driven photocatalysis on fluorine-doped TiO$_2$ powders by the creation of surface oxygen vacancies, Chem. Phys. Lett. 401 (2005) 579–584, https://doi.org/10.1016/j.cplett.2004.11.126.

[97] T.H. Wang, A.M. Navarrete-López, S. Li, D.A. Dixon, J.L. Gole, Hydrolysis of TiCl$_4$: initial steps in the production of TiO$_2$, J. Phys. Chem. A 114 (2010) 7561–7570, https://doi.org/10.1021/jp102020h.

[98] T. Sugimoto, X. Zhou, A. Muramatsu, Synthesis of uniform anatase TiO$_2$ nanoparticles by gel–sol method: 4. Shape control, J. Colloid Interface Sci. 259 (2003) 53–61, https://doi.org/10.1016/S0021-9797(03)00035-3.

[99] A. Hosseinnia, M. Keyanpour-Rad, M. Kazemzad, M. Pazouki, A novel approach for preparation of highly crystalline anatase TiO$_2$nanopowder from the agglomerates, Powder Technol. 190 (2009) 390–392, https://doi.org/10.1016/j.powtec.2008.08.019.

[100] A. Khitab, S. Ahmad, M.J. Munir, S.M. Kazmi, T. Arshad, R.A. Khushnood, Synthesis and applications of nanotitania particles: A review, Rev. Adv. Mater. Sci. 53 (2018) 90–105.

[101] Y. Masuda, K. Kato, Synthesis and phase transformation of TiO$_2$nano-crystals in aqueous solutions, J. Ceram. Soc. Jpn. 117 (2009) 373–376, https://doi.org/10.2109/jcersj2.117.373.

[102] D.A. Hanaor, C.C. Sorrell, Review of the anatase to rutile phase transformation, J. Mater. Sci. 46 (2011) 855–874, https://doi.org/10.1007/s10853-010-5113-0.

[103] M. Landmann, E. Rauls, W.G. Schmidt, The electronic structure and optical response of rutile, anatase and brookite TiO$_2$, J. Phys. Condens. Matter 24 (2012) 195503, https://doi.org/10.1088/0953-8984/24/19/195503.

[104] A. Mills, S. Le Hunte, An overview of semiconductor photocatalysis, J. Photochem. Photobiol. A 108 (1997) 1–35, https://doi.org/10.1016/S1010-6030(97)00118-4.

[105] R. Fagan, D.E. McCormack, D.D. Dionysiou, S.C. Pillai, A review of solar and visible light active TiO$_2$photocatalysis for treating bacteria, cyanotoxins and contaminants of emerging concern, Mater. Sci. Semicond. Process. 42 (2016) 2–14, https://doi.org/10.1016/j.mssp.2015.07.052.

[106] B. Ohtani, O.O. Prieto-Mahaney, D. Li, R. Abe, What is Degussa (Evonik) P25? Crystalline composition analysis, reconstruction from isolated pure particles and photocatalytic activity test, J. Photochem. Photobiol. A 216 (2010) 179–182, https://doi.org/10.1016/j.jphotochem.2010.07.024.

[107] J. Li, D. Xu, Tetragonal faceted-nanorods of anatase TiO$_2$ single crystals with a large percentage of active {100} facets, Chem. Commun. 46 (2010) 2301–2303, https://doi.org/10.1039/b923755k.

[108] W.J. Ong, L.L. Tan, S.P. Chai, S.T. Yong, A.R. Mohamed, Highly reactive {001} facets of TiO$_2$-based composites: synthesis, formation mechanism and characterization, Nanoscale 6 (2014) 1946–2008, https://doi.org/10.1039/c3nr04655a.

[109] X. Gong, A. Selloni, Reactivity of anatase TiO$_2$ nanoparticles: the role of the minority (001) surface, J. Phys. Chem. B 109 (2005) 19560–19562, https://doi.org/10.1021/jp055311g.

[110] G. Liu, H.G. Yang, J. Pan, Y.Q. Yang, G.Q. Lu, H.M. Cheng, Titanium dioxide crystals with tailored facets, Chem. Rev. 114 (2014) 9559–9612, https://doi.org/10.1021/cr400621z.

[111] Z. Niu, Y. Li, Removal and utilization of capping agents in nanocatalysis, Chem. Mater. 26 (2014) 72–83, https://doi.org/10.1021/cm4022479.

[112] N. Roy, Y. Sohn, D. Pradhan, Synergy of low-energy {101} and high-energy {001} TiO$_2$ crystal facets for enhanced photocatalysis, ACS Nano 7 (2013) 2532–2540, https://doi.org/10.1021/nn305877v.

[113] C. Dette, M.A. Pérez-Osorio, C.S. Kley, P. Punke, C.E. Patrick, P. Jacobson, F. Giustino, S.J. Jung, K. Kern, TiO$_2$ Anatase with a bandgap in the visible region, Nano Lett. 14 (2014) 6533–6538, https://doi.org/10.1021/nl503131s.

[114] M. Sayed, F. Pingfeng, H.M. Khan, P. Zhang, Effect of isopropanol on microstructure and activity of TiO$_2$ films with dominant {001} facets for photocatalytic degradation of bezafibrate, Int. J. Photoenergy (2014)https://doi.org/10.1155/2014/490264 Article ID 490264, 11 pages.

[115] H.G. Yang, G. Liu, S.Z. Qiao, C.H. Sun, Y.G. Jin, S.C. Smith, J. Zou, H.M. Cheng, G.Q. Lu, Solvothermal synthesis and photoreactivity of anatase TiO$_2$ nanosheets with dominant {001} facets, J. Am. Chem. Soc. 131 (2009) 4078–4083, https://doi.org/10.1021/ja808790p.

[116] Y. Dong, X. Fei, Z. Liu, Y. Zhou, L. Cao, Synthesis and photocatalytic redox properties of anatase TiO$_2$ single crystals, Appl. Surf. Sci. 394 (2017) 386–393, https://doi.org/10.1016/j.apsusc.2016.10.059.

[117] M. Maisano, M.V. Dozzi, M. Coduri, L. Artiglia, G. Granozzi, E. Selli, Unraveling the multiple effects originating the increased oxidative photoactivity of {001}-facet enriched anatase TiO$_2$, ACS Appl. Mater. Interfaces 8 (2016) 9745–9754, https://doi.org/10.1021/acsami.6b01808.

[118] Y. Liao, H. Zhang, W. Que, P. Zhong, F. Bai, Z. Zhong, Q. Wen, W. Chen, Activating the single-crystal TiO$_2$ nanoparticle film with exposed {001} facets, ACS Appl. Mater. Interfaces 5 (2013) 6463–6466, https://doi.org/10.1021/am401869e.

[119] M. Sayed, L.A. Shah, J.A. Khan, N.S. Shah, J. Nisar, H.M. Khan, P. Zhang, A.R. Khan, Efficient photocatalytic degradation of norfloxacin in aqueous media by hydrothermally synthesized immobilized TiO$_2$/Ti films with exposed {001} facets, J. Phys. Chem. A 120 (2016) 9916–9931, https://doi.org/10.1021/acs.jpca.6b09719.

[120] N. Fessi, M.F. Mohamed Nsib, L. Cardenas, C. Guillard, F. Dappozze, A. Houas, F. Parrino, L. Palmisano, G. Ledoux, D. Amans, Y. Chevalier, Surface and electronic features of fluorinated TiO$_2$ and their influence on the photocatalytic degradation of 1-methylnaphthalene, J. Phys. Chem. C 124 (2020) 11456–11468, https://doi.org/10.1021/acs.jpcc.0c01929.

[121] D. Zhang, G. Li, X. Yang, C.Y. Jimmy, A micrometer-size TiO$_2$ single-crystal photocatalyst with remarkable 80% level of reactive facets, Chem. Commun. 29 (2009) 4381–4383, https://doi.org/10.1039/b907963g.

[122] L.G. Devi, R. Kavitha, Review on modified N–TiO$_2$ for green energy applications under UV/visible light: selected results and reaction mechanisms, RSC Adv. 4 (2014) 28265–28299, https://doi.org/10.1039/c4ra03291h.

[123] X. Zhu, C. Jin, X.S. Li, J.L. Liu, Z.G. Sun, C. Shi, X. Li, A.M. Zhu, Photocatalytic formaldehyde oxidation over plasmonic Au/TiO$_2$ under visible light: Moisture indispensability and light enhancement, ACS Catal. 7 (2017) 6514–6524, https://doi.org/10.1021/acscatal.7b01658.

[124] E.L. Cates, Photocatalytic water treatment: so where are we going with this? Environ. Sci. Technol. 51 (2017) 757–758, https://doi.org/10.1021/acs.est.6b06035.

[125] P. Apopei, C. Catrinescu, C. Teodosiu, S. Royer, Mixed-phase TiO$_2$ photocatalysts: crystalline phase isolation and reconstruction, characterization and photocatalytic activity in the oxidation of 4-chlorophenol from aqueous effluents, Appl. Catal. B 160 (2014) 374–382, https://doi.org/10.1016/j.apcatb.2014.05.030.

[126] T. Kawahara, Y. Konishi, H. Tada, N. Tohge, J. Nishii, S. Ito, A patterned TiO_2 (anatase)/TiO_2 (rutile) bilayer-type photocatalyst: effect of the anatase/rutile junction on the photocatalytic activity, Angew. Int. Ed. 114 (2002) 2935–2937.

[127] J. Yu, C.Y. Jimmy, W. Ho, Z. Jiang, Effects of calcination temperature on the photocatalytic activity and photo-induced super-hydrophilicity of mesoporous TiO_2 thin films, New J. Chem. 26 (2002) 607–613, https://doi.org/10.1039/b200964a.

[128] H. Nakajima, T. Mori, Q. Shen, T. Toyoda, Photoluminescence study of mixtures of anatase and rutile TiO_2 nanoparticles: influence of charge transfer between the nanoparticles on their photoluminescence excitation bands, Chem. Phys. Lett. 409 (2005) 81–84, https://doi.org/10.1016/j.cplett.2005.04.093.

[129] D.C. Hurum, A.G. Agrios, K.A. Gray, T. Rajh, M.C. Thurnauer, Explaining the enhanced photocatalytic activity of Degussa P25 mixed-phase TiO_2 using EPR, J. Phys. Chem. B 107 (2003) 4545–4549, https://doi.org/10.1021/jp0273934.

[130] S. Shen, X. Wang, T. Chen, Z. Feng, Can Li, Transfer of photoinduced electrons in anatase–rutile TiO_2 determined by Time-Resolved Mid-Infrared Spectroscopy, J. Phys. Chem. C 118 (2014) 12661–12668 doi.org/10.1021/jp502912u.

[131] A.K. Mohapatra, J. Nayak, Anatase TiO_2 powder: Synthesis, characterization and application for photocatalytic degradation of 3,4-dihydroxy benzoic acid, Optik 156 (2018) 268–278, https://doi.org/10.1016/j.ijleo.2017.10.141.

[132] O. Chedeville, M. Debacq, C. Porte, Removal of phenolic compounds present in olive mill wastewaters by ozonation, Desalination 249 (2009) 865–869, https://doi.org/10.1016/j.desal.2009.04.014.

[133] Q. Wang, Z. Qiao, P. Jiang, J. Kuang, W. Liu, W. Cao, Hydrothermal synthesis and enhanced photocatalytic activity of mixed-phase TiO_2 powders with controllable anatase/rutile ratio, Solid State Sci. 77 (2018) 14–19, https://doi.org/10.1016/j.solidstatesciences.2018.01.003.

[134] R. Su, R. Bechstein, L. Sø, R.T. Vang, M. Sillassen, B. Esbjornsson, A. Palmqvist, F. Besenbacher, How the anatase-to-rutile ratio influences the photoreactivity of TiO_2, J. Phys. Chem. C115 (2011) 24287–24292, https://doi.org/10.1021/jp2086768.

[135] J. Schneider, M. Matsuoka, M. Takeuchi, J. Zhang, Y. Horiuchi, M. Anpo, D.W. Bahnemann, Understanding TiO_2 photocatalysis: mechanisms and materials, Chem. Rev. 114 (2014) 9919–9986, https://doi.org/10.1021/cr5001892.

[136] A.T. Kuvarega, R.W. Krause, B.B. Mamba, Nitrogen/palladium-codoped TiO_2 for efficient visible light photocatalytic dye degradation, J. Phys. Chem. C 115 (2011) 22110–22120, https://doi.org/10.1021/jp203744j.

[137] M.P. Blanco-Vega, J.L. Guzmán-Mar, L. Villanueva-Rodríguez, L. Maya-Treviño, L.L. Garza-Tovar, A. Hernández-Ramírez, L. Hinojosa-Reyes, Photocatalytic elimination of bisphenol A under visible light using Ni-doped TiO_2 synthesized by microwave assisted sol-gel method, Mater. Sci. Semicond. Process. 71 (2017) 275–282, https://doi.org/10.1016/j.mssp.2017.08.013.

[138] Q. Wang, C. Yang, G. Zhang, L. Hu, P. Wang, Photocatalytic Fe-doped TiO_2/PSF composite UF membranes: Characterization and performance on BPA removal under visible-light irradiation, Chem. Eng. J. 319 (2017) 39–47, https://doi.org/10.1016/j.cej.2017.02.145.

[139] H. Khan, I.K. Swati, Fe^{3+} doped anatase TiO_2 with d-d transition, oxygen vacancies and Ti^{3+} centers: synthesis, characterization, UV-vis photocatalytic and mechanistic studies, Ind. Eng. Chem. Res. 55 (2016) 6619–6633, https://doi.org/10.1021/acs.iecr.6b01104.

[140] D.P. Jaihindh, C.C. Chen, Y.P. Fu, Reduced graphene oxide-supported Ag-loaded Fe-doped TiO_2 for the degradation mechanism of methylene blue and its electrochemical properties, RSC Adv. 8 (2018) 6488–6501, https://doi.org/10.1039/c7ra13418e.

[141] Y.N. Tan, C.L. Wong, A.R. Mohamed, An Overview on the photocatalytic activity of nano-doped-TiO_2 in the degradation of organic pollutants, ISRN Mater. Sci. (2011) https://doi.org/10.5402/2011/261219 Article ID 261219, 18 pages.

[142] M. Wang, J. Ioccozia, L. Sun, C. Lin, Z. Lin, Inorganic-modified semiconductor TiO_2 nanotube arrays for photocatalysis, Energy Environ. Sci. 7 (2014) 2182–2202, https://doi.org/10.1039/c4ee00147h.

[143] L.F. Chiang, R.A. Doong, Cu-TiO_2 nanorods with enhanced ultraviolet-and visible-light photoactivity for bisphenol A degradation, J. Hazard. Mater. 277 (2014) 84–92, https://doi.org/10.1016/j.jhazmat.2014.01.047.

[144] E. Ioannidou, A. Ioannidi, Z. Frontistis, M. Antonopoulou, C. Tselios, D. Tsikritzis, I. Konstantinou, S. Kennou, D.I. Kondarides, D. Mantzavinos, Correlating the properties of hydrogenated titania to reaction kinetics and mechanism for the photocatalytic degradation of bisphenol A under solar irradiation, Appl. Catal. B 188 (2016) 65–76, https://doi.org/10.1016/j.apcatb.2016.01.060.

[145] S. Fukahori, H. Ichiura, T. Kitaoka, H. Tanaka, Capturing of bisphenol A photodecomposition intermediates by composite TiO_2–zeolite sheets, Appl. Catal. B 46 (2003) 453–462, https://doi.org/10.1016/S0926-3373(03)00270-4.

[146] L. Hlekelele, P.J. Franklyn, F. Dziike, S.H. Durbach, Novel synthesis of Ag decorated TiO_2 anchored on zeolites derived from coal fly ash for the photodegradation of bisphenol A, New J. Chem. 42 (2018) 1902–1912, https://doi.org/10.1039/c7nj02885g.

[147] X. Zhou, G. Liu, J. Yu, W. Fan, Surface plasmon resonance-mediated photocatalysis by noble metal-based composites under visible light, J. Mater. Chem. 22 (2012) 21337–21354, https://doi.org/10.1039/c2jm31902k.

[148] N. Zhou, V. López-Puente, Q. Wang, L. Polavarapu, I. Pastoriza-Santos, Q.H. Xu, Plasmon-enhanced light harvesting: Applications in enhanced photocatalysis, photodynamic therapy and photovoltaics, RSC Adv. 5 (2015) 29076–29097, https://doi.org/10.1039/c5ra01819f.

[149] R. Kavitha, S. Girish Kumar, Review on bimetallic-deposited TiO_2: Preparation methods, charge carrier transfer pathways and photocatalytic applications, Chem. Pap. 74 (2020) 717–756, https://doi.org/10.1007/s11696-019-00995-4.

[150] I. Tanabe, Y. Ozaki, Consistent changes in electronic states and photocatalytic activities of metal (Au, Pd, Pt)-modified TiO_2 studied by far-ultraviolet spectroscopy, Chem. Commun. 50 (2014) 2117–2119, https://doi.org/10.1039/c3cc48446g.

[151] M. Ye, J. Gong, Y. Lai, C. Lin, Z. Lin, High-efficiency photoelectrocatalytic hydrogen generation enabled by palladium quantum dots-sensitized TiO_2 nanotube arrays, J. Am. Chem. Soc. 134 (2012) 15720–15723, https://doi.org/10.1021/ja307449z.

[152] X. Zhou, N. Liu, P. Schmuki, Photocatalysis with TiO_2 nanotubes:"colorful" reactivity and designing site-specific photocatalytic centers into TiO_2 nanotubes, ACS Catal. 7 (2017) 3210–3235, https://doi.org/10.1021/acscatal.6b03709.

[153] X. He, W.G. Aker, M. Pelaez, Y. Lin, D.D. Dionysiou, H. Hwang, Assessment of Nitrogen-Fluorine-codoped TiO_2 under visible light for degradation of BPA: implication for field remediation, J. Photochem. Photobiol. A (2015) https://doi.org/10.1016/j.jphotochem.2015.08.014.

[154] T. Xu, M. Wang, T. Wang, Effects of N doping on the microstructures and optical properties of TiO_2, J. Wuhan Univ. Technol. Mater. Sci. Ed. 34 (2019) 55–63, https://doi.org/10.1007/s11595-019-2014-1.

[155] C. Di Valentin, G. Pacchioni, A. Selloni, S. Livraghi, E. Giamello, Characterization of paramagnetic species in N-doped TiO_2 powders by EPR spectroscopy and DFT calculations, J. Phys. Chem. B 109 (2005) 11414–11419, https://doi.org/10.1021/jp051756t.

[156] S. Livraghi, M.C. Paganini, E. Giamello, A. Selloni, C. Di Valentin, G. Pacchioni, Origin of photoactivity of nitrogen-doped titanium dioxide under visible light, J. Am. Chem. Soc. 128 (2006) 15666–15671, https://doi.org/10.1021/ja064164c.

[157] A.R. Puigdollers, P. Schlexer, S. Tosoni, G. Pacchioni, Increasing oxide reducibility: The role of metal/oxide interfaces in the formation of oxygen vacancies, ACS Catal. 7 (2017) 6493–6513, https://doi.org/10.1021/acscatal.7b01913.

[158] G. Li, L. Li, J. Boerio-Goates, B.F. Woodfield, High purity anatase TiO_2 nanocrystals: near room-temperature synthesis, grain growth kinetics, and surface hydration chemistry, J. Am. Chem. Soc. 127 (2005) 8659–8666, https://doi.org/10.1021/ja050517g.

[159] W. Yu, X. Liu, L. Pan, J. Li, J. Liu, J. Zhang, P. Li, C. Chen, Z. Sun, Enhanced visible light photocatalytic degradation of methylene blue by F-doped TiO_2, Appl. Surf. Sci. 319 (2014) 107–112, https://doi.org/10.1016/j.apsusc.2014.07.038.

[160] J. Zhao, W. Li, X. Li, X. Zhang, Low temperature synthesis of water dispersible F-doped TiO_2 nanorods with enhanced photocatalytic activity, RSC Adv. 7 (2017) 21547–21555, https://doi.org/10.1039/c7ra00850c.

[161] E.B. Simsek, B. Kilic, M. Asgin, A. Akan, Graphene oxide based heterojunction TiO_2–ZnO catalysts with outstanding photocatalytic performance for bisphenol-A, ibuprofen and flurbiprofen, J. Ind. Eng. Chem. 59 (2018) 115–126, https://doi.org/10.1016/j.jiec.2017.10.014.

[162] D. Chen, H. Zhang, Y. Liu, J. Li, Graphene and its derivatives for the development of solar cells, photoelectrochemical, and photocatalytic applications, Energy Environ. Sci. 6 (2013) 1362–1387, https://doi.org/10.1039/c3ee23586f.

[163] X. Qian, M. Ren, M. Fang, M. Kan, D. Yue, Z. Bian, H. Li, J. Jia, Y. Zhao, Hydrophilic mesoporous carbon as iron (III)/(II) electron shuttle for visible light enhanced Fenton-like degradation of organic pollutants, Appl. Catal. B 231 (2018) 108–114, https://doi.org/10.1016/j.apcatb.2018.03.016.

[164] S.A.S. Shah, A.R. Park, K. Zhang, J.H. Park, P.J. Yoo, Green synthesis of biphasic TiO_2–reduced graphene oxide nanocomposites with highly enhanced photocatalytic activity, ACS Appl. Mater. Interfaces 4 (2012) 3893–3901, https://doi.org/10.1021/am301287m.

[165] K. Li, J. Xiong, T. Chen, L. Yan, Y. Dai, D. Song, Y. Lv, Z. Zeng, Preparation of graphene/TiO_2 composites by nonionic surfactant strategy and their simulated sunlight and visible light photocatalytic activity towards representative aqueous POPs degradation, J. Hazard. Mater. 250 (2013) 19–28, https://doi.org/10.1016/j.jhazmat.2013.01.069.

[166] D. Liang, C. Cui, H. Hu, Y. Wang, S. Xu, B. Ying, P. Li, B. Lu, H. Shen, One-step hydrothermal synthesis of anatase TiO_2/reduced graphene oxide nanocomposites with enhanced photocatalytic activity, J. Alloys Compd. 582 (2014) 236–240, https://doi.org/10.1016/j.jallcom.2013.08.062.

[167] L.W. Zhang, H.B. Fu, Y.F. Zhu, Efficient TiO_2 photocatalysts from surface hybridization of TiO_2 particles with graphite-like carbon, Adv. Funct. Mater. 18 (2008) 2180–2189, https://doi.org/10.1002/adfm.200701478.

[168] L. Yang, S. Luo, Y. Li, Y. Xiao, Q. Kang, Q. Cai, High efficient photocatalytic degradation of p-nitrophenol on a unique Cu_2O/TiO_2 p-n heterojunction network catalyst, Environ. Sci. Technol. 44 (2010) 7641–7646, https://doi.org/10.1021/es101711k.

[169] X. Deng, H. Zhang, Q. Ma, Y. Cui, X. Cheng, X. Li, M. Xie, Q. Cheng, Fabrication of p-NiO/n-TiO_2 nano-tube arrays photoelectrode and its enhanced photocatalytic performance for degradation of 4-chlorophenol, Sep. Purif. Technol. 186 (2017) 1–9, https://doi.org/10.1016/j.seppur.2017.04.052.

[170] Q. Li, H. Qin, H. Zhao, X. Zhao, X. Cheng, W. Fan, Facile fabrication of a BiOI/TiO_2 p-n junction via a surface charge-induced electrostatic self-assembly method, Appl. Surf. Sci. 457 (2018) 59–68, https://doi.org/10.1016/j.apsusc.2018.06.222.

[171] D. Sánchez-Rodríguez, M.G. Medrano, H. Remita, V. Escobar-Barrios, Photocatalytic properties of BiOCl-TiO_2 composites for phenol photodegradation, J. Environ. Chem. Eng. 6 (2018) 1601–1612, https://doi.org/10.1016/j.jece.2018.01.061.

[172] J. Park, Visible and near infrared light active photocatalysis based on conjugated polymers, J. Ind. Eng. Chem. 51 (2017) 27–43, https://doi.org/10.1016/j.jiec.2017.03.022.

[173] F. Torki, H. Faghihian, Visible light degradation of naproxen by enhanced photocatalytic activity of NiO and NiS, scavenger study and focus on catalyst support and magnetization, Photochem. Photobiol. 94 (2018) 491–502, https://doi.org/10.1111/php.12906.

[174] T.J. Brooms, B. Otieno, M.S. Onyango, A. Ochieng, Photocatalytic degradation of p-cresol using TiO_2/ZnO hybrid surface capped with polyaniline, J. Environ. Sci. Health A 53 (2018) 99–107, https://doi.org/10.1080/10934529.2017.1377583.

[175] E.A. Serna-Galvis, J. Silva-Agredo, A.L. Giraldo, O.A. Flórez, R.A. Torres-Palma, Comparison of route, mechanism and extent of treatment for the degradation of a β-lactam antibiotic by TiO_2 photocatalysis, sonochemistry, electrochemistry and the

photo-Fenton system, Chem. Eng. J. 284 (2016) 953–962, https://doi.org/10.1016/j.cej.2015.08.154.

[176] G. Zhang, Y. Sun, C. Zhang, Z. Yu, Decomposition of acetaminophen in water by a gas phase dielectric barrier discharge plasma combined with TiO_2-rGO nanocomposite: Mechanism and degradation pathway, J. Hazard. Mater. 323 (2017) 719–729, https://doi.org/10.1016/j.jhazmat.2016.10.008.

[177] D. Meroni, M. Jiménez-Salcedo, E. Falletta, B.M. Bresolin, C.F. Kait, D.C. Boffito, C. Pirola, Sonophotocatalytic degradation of sodium diclofenac using low power ultrasound and micro sized TiO_2, Ultrason. Sonochem. 67 (2020) 105123, https://doi.org/10.1016/j.ultsonch.2020.105123.

[178] M. Klavarioti, D. Mantzavinos, D. Kassinos, Removal of residual pharmaceuticals from aqueous systems by advanced oxidation processes, Environ. Int. 35 (2009) 402–417, https://doi.org/10.1016/j.envint.2008.07.009.

[179] S. Chakma, V.S. Moholkar, Intensification of wastewater treatment using sono-hybrid processes: An overview of mechanistic synergism, Indian Chem. Eng. 57 (2015) 359–381, https://doi.org/10.1080/00194506.2015.1026948.

[180] C. Minero, M. Lucchiari, D. Vione, V. Maurino, Fe(lll)-enhanced sonochemical degradation of methylene blue in aqueous solution, Environ. Sci. Technol. 39 (2005) 8936–8942, https://doi.org/10.1021/es050314s.

[181] L. Yang, J.F. Rathman, L.K. Weavers, Sonochemical degradation of alkylbenzene sulfonate surfactants in aqueous mixtures, J. Phys. Chem. B 110 (2006) 18385–18391, https://doi.org/10.1021/jp062327d.

[182] J. Cheng, C.D. Vecitis, H. Park, B.T. Mader, M.R. Hoffmann, Sonochemical degradation of perfluorooctane sulfonate (PFOS) and perfluorooctanoate (PFOA) in landfill groundwater: environmental matrix effects, Environ. Sci. Technol. 42 (2008) 8057–8063, https://doi.org/10.1021/es8013858.

[183] J. Madhavan, F. Grieser, M. Ashokkumar, Kinetics of the sonophotocatalytic degradation of orange G in presence of Fe^{3+}, Water Sci. Technol. 60 (2009) 2195–2202, https://doi.org/10.2166/wst.2009.631.

[184] S. Dalhatou, C. Pétrier, H. Massaï, P.M. Kouotou, S. Laminsi, S. Baup, Degradation of endocrine disrupting chemical nonylphenol in aqueous milieu using high frequency ultrasound, Int. J. Water Wastewater Treat 2 (2016)https://doi.org/10.16966/2381-5299.129.

[185] S. Dalhatou, S. Laminsi, C. Pétrier, S. Baup, Competition in sonochemical degradation of naphthol blue black: Presence of an organic (nonylphenol) and a mineral (bicarbonate ions) matrix, J. Environ. Chem. Eng. 7 (2019) 102819, https://doi.org/10.1016/j.jece.2018.102819.

[186] S. Dalhatou, C. Pétrier, S. Laminsi, S. Baup, Sonochemical removal of naphthol blue black azo dye: influence of parameters and effect of mineral ions, Int. J. Environ. Sci. Technol. 12 (2015) 35–44, https://doi.org/10.1007/s13762-013-0432-8.

[187] T. Luo, Z. Ai, L. Zhang, $Fe@Fe_2O_3$ core-shell nanowires as iron reagent. 4.Sono-Fenton degradation of pentachlorophenol and the mechanism analysis, J. Phys. Chem. C 112 (2008) 8675–8681, https://doi.org/10.1021/jp800926n.

[188] Z. He, S. Song, H. Zhou, H. Ying, J. Chen, C.I. Reactive Black 5 decolorization by combined sonolysis and ozonation, Ultrason. Sonochem. 14 (2006) 298–304, https://doi.org/10.1016/j.ultsonch.2006.09.002.

[189] R. Vinu, G. Madras, Kinetics of sonphotocatalytic degradation of anionic dyes with nano-TiO_2, Environ. Sci. Technol. 43 (2009) 473–479, https://doi.org/10.1021/es8025648.

[190] C.G. Joseph, G.L. Puma, A. Bono, D. Krishnaiah, Sonophotocatalysis in advanced oxidation process: A short review, Ultrason. Sonochem. 16 (2009) 583–589, https://doi.org/10.1016/j.ultsonch.2009.02.002.

[191] M. Jagannathan, F. Grieser, M. Ashokkumar, Sonophotocatalytic degradation of paracetamol using TiO_2 and Fe^{3+}, Sep. Purif. Technol. 103 (2013) 114–118, https://doi.org/10.1016/j.seppur.2012.10.003.

[192] R.A. Torres, J.I. Nieto, E. Combet, C. Pétrier, C. Pulgarin, Influence of TiO_2 concentration on the synergistic effect between photocatalysis and high-frequency ultrasound for organic pollutant mineralization in water, Appl. Catal. B 80 (2008) 168–175, https://doi.org/10.1016/j.apcatb.2007.11.013.

[193] J. Madhavan, P.S.S. Kumar, S. Anandan, M. Zhou, F. Grieser, M. Ashokkumar, Ultrasound assisted photocatalytic degradation of diclofenac in an aqueous environment, Chemosphere 80 (2010) 747–752, https://doi.org/10.1016/j.chemosphere.2010.05.018.

[194] J. Madhavan, P.S.S. Kumar, S. Anandan, F. Grieser, M. Ashokkumar, Sonophotocatalytic degradation of monocrotophos using TiO_2 and Fe^{3+}, J. Hazard. Mater. 177 (2010) 944–949, https://doi.org/10.1016/j.jhazmat.2010.01.009.

[195] S. Adish Kumar, G.S. Sree Lekshmi, J. Rajesh Banu, I. Tae Yeom, Synergistic degradation of hospital wastewater by solar/TiO_2/Fe^{2+}/H_2O_2 process, Water Qual. Res. J. Can. 49 (2014) 223–233, https://doi.org/10.2166/wqrjc.2014.026.

[196] G. Selvabharathi, S. Adishkumar, S. Jenefa, G. Ginni, J.R. Banu, I.T. Yeom, Combined homogeneous and heterogeneous advanced oxidation process for the treatment of tannery wastewaters, J. Water Reuse Desal. 6 (2016) 59–71, https://doi.org/10.2166/wrd.2015.139.

[197] O.M. Ama, O.A. Arotiba, Exfoliated graphite/titanium dioxide for enhanced photoelectrochemical degradation of methylene blue dye under simulated visible light irradiation, J. Electroanal. Chem. 803 (2017) 157–164, https://doi.org/10.1016/j.jelechem.2017.09.015.

[198] X. Cheng, Q. Cheng, X. Deng, P. Wang, H. Liu, A facile and novel strategy to synthesize reduced TiO_2 nanotubes photoelectrode for photoelectrocatalytic degradation of diclofenac, Chemosphere 144 (2016) 888–894, https://doi.org/10.1016/j.chemosphere.2015.09.070.

[199] H. Jiang, Q. Wang, S. Zang, J. Li, Q. Wang, Enhanced photoactivity of Sm, N, P-tridoped anatase-TiO_2nano-photocatalyst for 4-chlorophenol degradation under sunlight irradiation, J. Hazard. Mater. 261 (2013) 44–54, https://doi.org/10.1016/j.jhazmat.2013.07.016.

[200] A.M. Abdullah, N.J. Al-Thani, K. Tawbi, H. Al-Kandari, Carbon/nitrogen-doped TiO_2: New synthesis route, characterization and application for phenol degradation, Arab. J. Chem. 9 (2016) 229–237, https://doi.org/10.1016/j.arabjc.2015.04.027.

[201] S.Y. Mendiola-Alvarez, J.L. Guzmán-Mar, G. Turnes-Palomino, F. Maya-Alejandro, A. Hernández-Ramírez, L. Hinojosa-Reyes, UV and visible activation of Cr (III)-doped TiO_2 catalyst prepared by a microwave-assisted sol–gel method during MCPA degradation, Environ. Sci. Pollut. Res. 24 (2017) 12673–12682, https://doi.org/10.1007/s11356-016-8034-x.

[202] Z. Huang, P. Wu, B. Gong, X. Zhang, Z. Liao, P.C. Chiang, X. Hu, L. Cui, Immobilization of visible light-sensitive (N, Cu) co-doped TiO_2 onto rectorite for photocatalytic degradation of p-chlorophenol in aqueous solution, Appl. Clay Sci. 142 (2017) 128–135, https://doi.org/10.1016/j.clay.2016.10.010.

[203] A.H. Khavar, G. Moussavi, A.R. Mahjoub, M. Satari, P. Abdolmaleki, Synthesis and visible-light photocatalytic activity of In, S-TiO_2@rGO nanocomposite for degradation and detoxification of pesticide atrazine in water, Chem. Eng. J. 345 (2018) 300–311, https://doi.org/10.1016/j.cej.2018.03.095.

[204] T. Boningari, S.N. Inturi, M. Suidan, P.G. Smirniotis, Novel one-step synthesis of nitrogen-doped TiO_2 by flame aerosol technique for visible-light photocatalysis: Effect of synthesis parameters and secondary nitrogen (N) source, Chem. Eng. J. 350 (2018) 324–334, https://doi.org/10.1016/j.cej.2018.05.122.

[205] M. Crişan, D. Mardare, A. Ianculescu, N. Drăgan, I. Niţoi, D. Crişan, M. Voicescu, L. Todan, P. Oancea, C. Adomniţei, M. Dobromir, Iron doped TiO_2 films and their photoactivity in nitrobenzene removal from water, Appl. Surf. Sci. 455 (2018) 201–215, https://doi.org/10.1016/j.apsusc.2018.05.124.

[206] M. Lu, C. Shao, K. Wang, N. Lu, X. Zhang, P. Zhang, M. Zhang, X. Li, Y. Liu, p-$MoO3$ Nanostructures/n-TiO_2 nanofiberheterojunctions: Controlled fabrication and enhanced photocatalytic properties, ACS Appl. Mater. Interfaces 6 (2014) 9004–9012, https://doi.org/10.1021/am5021155.

[207] X. Hao, M. Li, L. Zhang, K. Wang, C. Liu, Photocatalyst TiO_2/WO_3/GO nanocomposite with high efficient photocatalytic performance for BPA degradation under visible light and solar light illumination, J. Ind. Eng. Chem. 55 (2017) 140–148, https://doi.org/10.1016/j.jiec.2017.06.038.

[208] Y. Zhao, C. Tao, G. Xiao, H. Su, Controlled synthesis and wastewater treatment of Ag_2O/TiO_2 modified chitosan-based photocatalytic film, RSC Adv. 7 (2017) 11211–11221, https://doi.org/10.1039/c6ra27295a.

[209] K. Park, I. Ali, J.O. Kim, Photodegradation of perfluorooctanoic acid by graphene oxide-deposited TiO_2 nanotube arrays in aqueous phase, J. Environ. Manag. 218 (2018) 333–339, https://doi.org/10.1016/j.jenvman.2018.04.016.

[210] B. MirzaHedayat, M. Noorisepehr, E. Dehghanifard, A. Esrafili, R. Norozi, Evaluation of photocatalytic degradation of 2,4-dinitrophenol from synthetic wastewater using Fe_3O_4@SiO_2@TiO_2/rGO magnetic nanoparticles, J. Mol. Liq. 262 (2018) 404–411, https://doi.org/10.1016/j.molliq.2018.05.102.

[211] Y. Gong, Y. Wu, Y. Xu, L. Li, C. Li, X. Liu, L. Niu, All-Solid-State Z-scheme CdTe/TiO_2 heterostructure photocatalysts with enhanced visible-light photocatalytic degradation of antibiotic waste water, Chem. Eng. J. 350 (2018) 257–267, https://doi.org/10.1016/j.cej.2018.05.186.

[212] M. Khodadadi, M.H. Ehrampoush, M.T. Ghaneian, A. Allahresani, A.H. Mahvi, Synthesis and characterizations of $FeNi_3$@SiO_2@TiO_2 nanocomposite and its application in photo-catalytic degradation of tetracycline in simulated wastewater, J. Mol. Liq. 255 (2018) 224–232, https://doi.org/10.1016/j.molliq.2017.11.137.

[213] X. Hu, Z. Sun, J. Song, G. Zhang, C. Li, S. Zheng, Synthesis of novel ternary heterogeneous $BiOCl$/TiO_2/sepiolite composite with enhanced visible-light-induced photocatalytic activity towards tetracycline, J. Colloid Interface Sci. 533 (2019) 238–250, https://doi.org/10.1016/j.jcis.2018.08.077.

[214] M. Ai, W. Qin, T. Xia, Y. Ye, X. Chen, P. Zhang, Photocatalytic degradation of 2,4 dichlorophenol by TiO_2 intercalated talc nanocomposite, Int. J. Photoenergy (2019) https://doi.org/10.1155/2019/1540271 Article ID 1540271, 11p.